AWARD NUMBER: W81XWH-13-1-0171

TITLE: Development of Diazaquinomycin Class Antibiotics for the Treatment of Drug-Resistant TB Infections

PRINCIPAL INVESTIGATOR: Professor Scott Franzblau

CONTRACTING ORGANIZATION: University of Illinois at Chicago
Chicago, IL 60612-7231

REPORT DATE: October 2016

TYPE OF REPORT: Final Report

PREPARED FOR: U.S. Army Medical Research and Materiel Command
Fort Detrick, Maryland 21702-5012

REPORT DOCUMENTATION PAGE

Form Approved
OMB No. 0704-0188

1. REPORT DATE *(DD-MM-YYYY)*	**2. REPORT TYPE**	**3. DATES COVERED** *(From - To)*
October 2016	Final Report	15July2013 - 14July2016

4. TITLE AND SUBTITLE
Development of Diazaquinomycin Class Antibiotics for the Treatment of Drug-Resistant TB Infections

5a. CONTRACT NUMBER
W81XWH-13-1-0171

5b. GRANT NUMBER

5c. PROGRAM ELEMENT NUMBER

6. AUTHOR(S)
Scott Franzblau, Ph.D.; sgf@uic.edu.

Larry Klein, Ph.D.; llk@uic.edu

Email: sgf@uic.edu

5d. PROJECT NUMBER

5e. TASK NUMBER

5f. WORK UNIT NUMBER

7. PERFORMING ORGANIZATION NAME(S) AND ADDRESS(ES)
University of Illinois at Chicago
809 S. Marshfield Rm 520
Chicago, IL 60612-4305

8. PERFORMING ORGANIZATION REPORT NUMBER

9. SPONSORING / MONITORING AGENCY NAME(S) AND ADDRESS(ES)
U.S. Army Medical Research and Materiel Command
Fort Derrick, Maryland 21702-5012

10. SPONSOR/MONITOR'S ACRONYM(S)

11. SPONSOR/MONITOR'S REPORT NUMBER(S)

12. DISTRIBUTION / AVAILABILITY STATEMENT
Approved for Public Release; distribution unlimited

13. SUPPLEMENTARY NOTES

14. ABSTRACT

In the current proposal, we utilize a panel of TB tests to generate potential therapeutics that target *M. tuberculosis* growth. The source of therapeutics is our growing library of aquatic bacteria, since these unique microorganisms have the proven ability to produce unique molecules that have a relatively high potential for use as medicines. This model has been successful in just a few years of its implementation, as recently we have licensed a novel anti-TB natural product to B&C Biopharm in South Korea. In addition, from screening our library of compounds against non-replicating TB, we have identified eight aquatic bacterial strains that target non-replicating TB, all of which do not exhibit signs of known antibiotic classes. From this screening we have also identified a promising class of antibiotics (DAQ) that appear to selectively target mycobacteria with drug-like potency. In this proposal we will 1) identify the antibiotics from the eight actinomycete strains that target non-replicating *M. tuberculosis* and evaluate their ability to be viable TB leads, 2) synthesize and evaluate the DAQ antibiotics for their potential to become viable drugs, and 3) identify how the DAQ antibiotics work in the cell. The Partnering PI Option poises us to fuse small molecule chemistry, aquatic microbiology, and molecular biology with drug discovery to utilize novel small molecules that target NR *M. tuberculosis*. This proposal utilizes our capacity to identify antibiotics from libraries of aquatic actinomycete strains, and thoroughly profile hits and leads with respect to anti-TB potency, selectivity, and drug-like behavior.

15. SUBJECT TERMS

Nothing listed

16. SECURITY CLASSIFICATION OF:			**17. LIMITATION OF ABSTRACT**	**18. NUMBER OF PAGES**	**19a. NAME OF RESPONSIBLE PERSON**
a. REPORT	**b. ABSTRACT**	**c. THIS PAGE**			USAMRMC
U	U	U	UU	64	**19b. TELEPHONE NUMBER** *(include area code)*

Table of Contents

1) Introduction

In 2013 the World Health Organization estimated that there were 1.5 million deaths as a result of tuberculosis (TB) infection, with 9.0 million new cases reported. The most significant threat to our population is multidrug- and extensively drug-resistant strains of *M. tuberculosis* (MDR- and XDR-TB), which are resistant to first and second line drug regimens and resulted in 210,000 fatalities in 2013 (of 480,000 reported infections).[1] A major deficiency of current TB treatment is its long duration, which is necessary to eliminate a persistent subpopulation of slow-growing or non-replicating cells. Importantly, TB is a disease that affects predominantly underprivileged populations in the developing world and the emergence of drug-resistant forms coupled with the ease at which TB spreads between humans has solidified it as a pathogen of global concern. The current award focuses on the discovery of new TB leads from aquatic actinomycete bacteria and the development of the diazaquinomycin class of compounds as TB leads.

2) **Keywords:** tuberculosis, actinomycete, antibiotic, drug discovery

3) Overall Project Summary:

Task 1. Synthesis of DAQA and identification of secondary metabolites that target *M. tuberculosis* $H_{37}Rv$. As summarized in the 2014 and 2015 annual reports, we successfully completed the total synthesis of DAQA (Figure 1, **Task 1 i**) to generate sufficient material for *in vitro* and *in vivo* PK and ADME studies.

Additionally, according to **Task 2 i & ii**, we determined the MIC of DAQA and analogs

Figure 1. Total synthesis of DAQA.

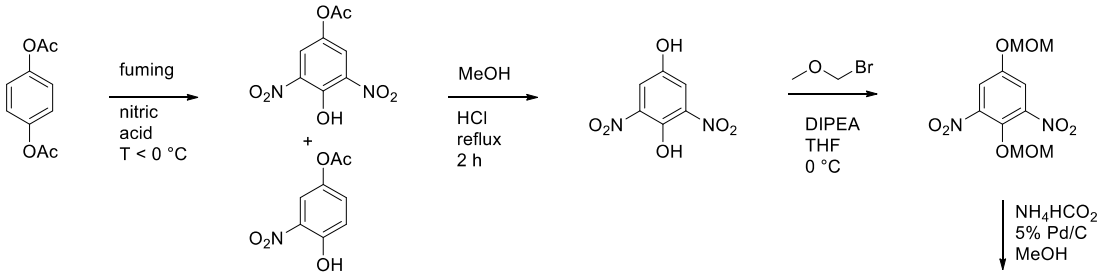

Figure 2. Summary of bioactive structures from TB-active strains.

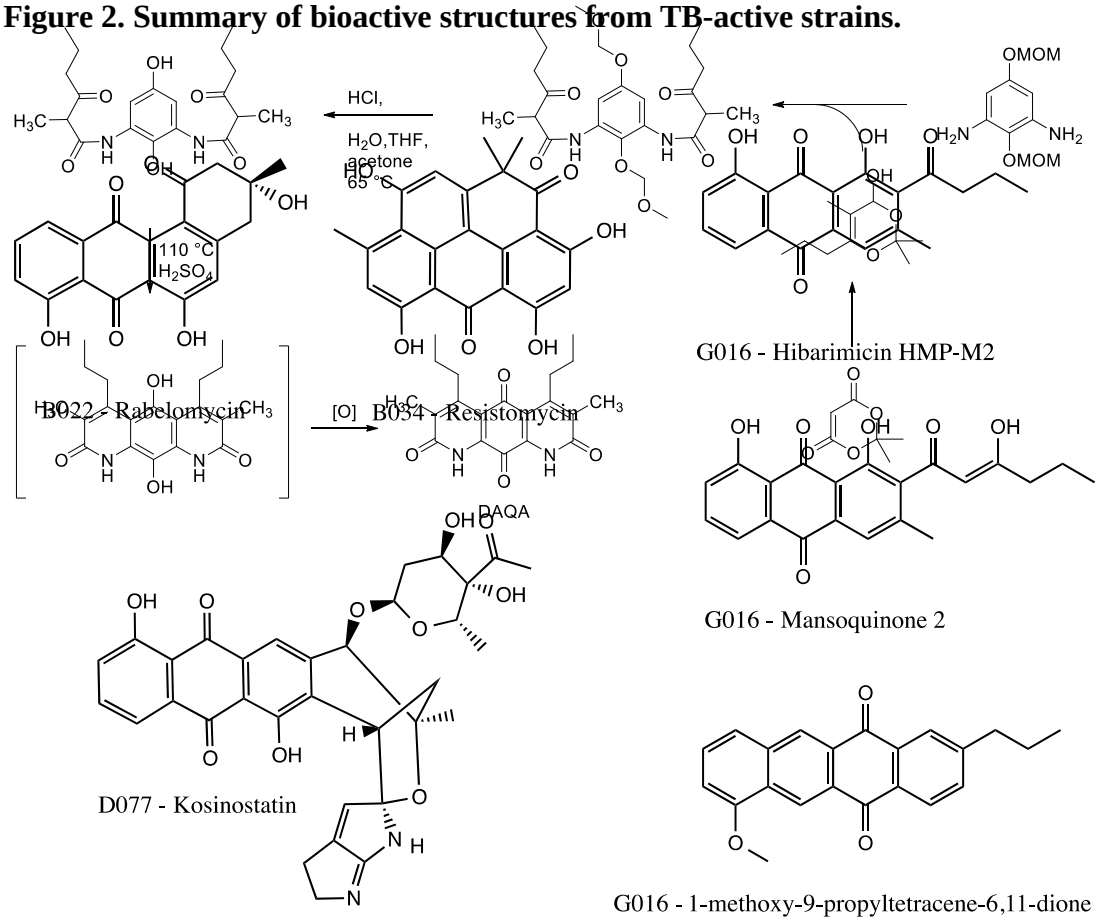

against M. tuberculosis H37Rv and a panel of diverse bacterial pathogens. *This work was*

presented in detail in previous DOD annual reports. The summary of these screening efforts is as follows. We isolated and identified six major specialized metabolites from eight strains (**Task 1 ii**) that exhibited antibiotic activity toward *M. tuberculosis*. Most activities were accompanied by toxicity toward eukaryotic cells, a common phenomenon in the search for natural products from nature. In each of these cases, we deprioritized further characterization of biological activity. A summary of these structures are in Figure 2. Strains D076, G017, and Z002 lost activity during the fractionation process, potentially due to compound degradation. Much deeper efforts are needed to understand the causes for this loss in bioactivity. From strain G039, in addition to identifying four bioactive angucyclines, we reported the rare isolation and characterization of a novel pimarane diterpene from an actinomycete strain, one of approximately twenty actinomycete-derived diterpenes of the 12,000 reported to date; this was a particularly rare find. This past year (since the 2015 report), we published these results in the journal Marine Drugs (Figure 3).[2]

Figure 3. Bioactive structures from G039.

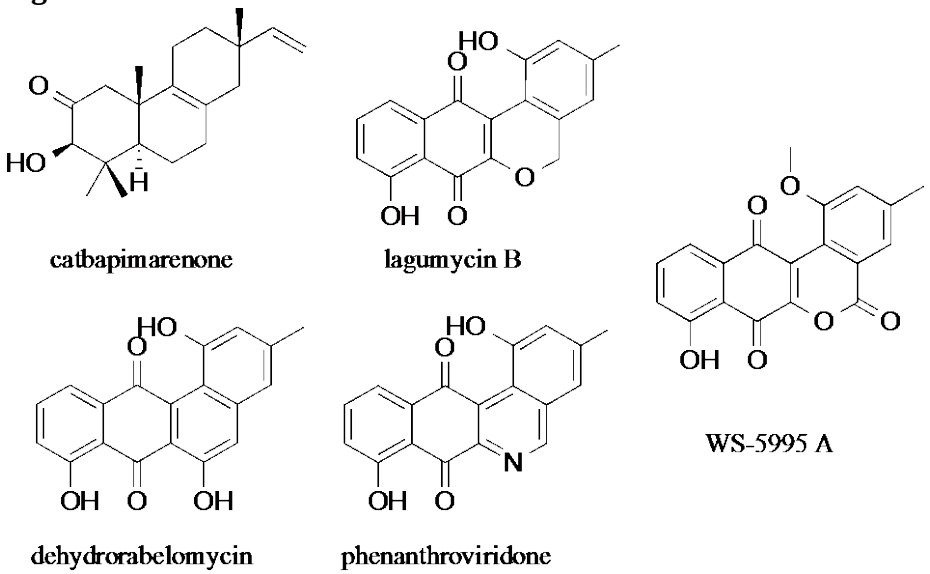

Task 2. Determine potential of DAQA and other leads for in vivo efficacy.

In vivo evaluation of diazaquinomycin A (**Task 2 iii**). As stated in the 2015 annual report, we performed an initial tolerance assessment of DAQA as our first *in vivo* study and the compound exhibited no qualitatively detectable ill effect and was well tolerated when dosed daily by oral gavage at 100 mg/kg for five days in uninfected mice. While it is possible this difference was due to limited oral bioavailability, our Caco-2 data predicted otherwise. This past year we further assessed the *in vivo* capacity of DAQA.

We assessed the pharmacokinetics (PK) of DAQA in mouse lungs and plasma. Dosing twenty-four seven- to ten-week old male Balb/c mice with DAQA followed by analysis at half-, one-, two-, and four-hour time points resulted in observation of DAQA in lungs and plasma by LC-MS. The greatest concentrations were seen at two hours, though none of the time points resulted in concentrations that could be observed above the LC-MS limit of quantitation (LOQ). Interestingly, the internal standard, tetramethyl-diazaquinomycin, was also frequently below the LOQ when extracted from matrices but not when injected in clean ACN indicating that DAQA solubility was likely a cause. In addition to dosing of 100 mg/kg in 10 µL/kg vehicle by oral gavage, half of the

mice were dosed at 50 mg/kg in 5 µL/kg vehicle intraperitoneally. Similar to the toxicity study, mice dosed by oral gavage remained healthy throughout all PK time points, while acute toxicity evidenced by hunched posture, closed eyes, decreased activity, and a rough coat followed dosing by IP.

Despite the lack of conclusive data in the PK study, we progressed to *in vivo* studies of DAQA to examine efficacy in TB-infected mice in collaboration with Carolyn Shoen in the lab of Michael Cynamon. Unfortunately, the vehicle was found to be toxic when two control mice died after four days, so the experiment failed to produce conclusive results.

Task 3. Studies toward Mechanism of Action of DAQA. (**Task 3 i-iii**) In the 2014 annual report, we stated that DAQA did not significantly inhibit the activity of thymidylate synthase A, as was reported previously in the literature (for other Gram—positive bacteria, not TB). This finding was significant, as the research community long thought ThyA was a major target of the diazaquinomycin compound class and we showed that at least in TB, this was likely not the case. In the 2015 annual report, we detailed our efforts to generate resistant mutants in *M. tuberculosis* toward DAQA. We also discussed the screening of an entire clone library of overexpressed genes in *M. tuberculosis*, while one clone (TOE Rv0953c) showed a definite shift towards resistance to the diazaquinomycin compound class, which was more pronounced after induction of expression (a continuation of work from **Task 3 ii,** as reported in detail in DOD 2015 Annual Report). This clone was of the F420-bearing enzymes class that are absent in humans, not well represented in prokaryotes, but present extensively in mycobacteria, providing an attractive, although non-essential, target. Hereafter, we will present a summary of the many experiments that performed in the past year aimed at identifying the target of DAQA (Figure 4; summary of **Task 3 i-iii**)).

Figure 4. Summary of experiments performed to determine DAQA mechanisms of action.

	Mechanism of Action (MOA)/Resistance			
	oxidative stress	F_{420} biosynthesis	pyrimidine biosynthesis	efflux (MmpL5)
Experiment				
ITR mutants (rCLF1 and rCLF4)	✓	✓	✓	✓
transcription profile	✓			
overexpression mutant screen		✓		
ATP/ETC screen	◇			
F_{420} biosynthesis mutants		⊗		
***Pyr* and *upp* mutants; uracil supplementation**			⊗	
MmpL5 regulator (Rv0678) mutants				⊗

Having eliminated the possibility that DAQA targets thymidylate synthase as it had been reported for other organisms, we set out to establish the mechanism of inhibition in *M. tuberculosis*. Initially, we attempted to directly capture a molecular target of DAQA using the DARTS method, but that proved unfruitful (**Task 3 iii**).[3, 4] Later, approaches using overexpression mutant screening, transcription profiling, and a screening against clofazimine-resistant mutant strains (rCLF1 and rCLF4) revealed potential mechanisms of action involving oxidative stress, F_{420} biosynthesis, pyrimidine biosynthesis, and MmpL5 efflux. We set out to confirm each of these with additional targeted experiments. Although we were unable to confidently identify a singular

molecular target using the experiments as detailed herein we gained potential evidence suggesting inhibition by oxidative stress (Figure 5).

Table 1. Resistance of Rv0953c, Rv2486, and Rv3500c *M. tuberculosis* OE mutants to **3.**

Strain	Rifampin MIC (μM)		DAQ-A MIC (μM)		Fold change from WT[a]	
	Uninduced	Induced	Uninduced	Induced	Uninduced	Induced
Wild-type	0.0026	0.00	0.24	0.20	1.0	1.0
TOE Rv0953c	0.0044	0.01	0.91	1.3	3.8	6.5
TOE Rv2486	0.0017	0.00	0.40	0.42	1.7	2.1
TOE Rv3500c	0.0016	*nd*	1.4	*nd*	5.8	*nd*

[a]fold change as compared to wild-type is given as a measure of resistance. *nd* – not determined; the growth of the Rv3500c OE strain was insufficient to determine MIC in the presence of ATc.

Following overexpression library screening discussed in the 2015 annual report and in the preceeding paragraphs, the Rv0953c OE mutant exhibited a shift toward resistance to DAQA, which was more pronounced after induction of expression. A second clone overexpressing Rv3500c showed resistance in uninduced conditions but induction of expression was detrimental to growth. The third clone selected for follow-up, a Rv2486 OE mutant, only showed a two-fold shift in MIC. This was deemed insignificant and the mutant deprioritized (Table 1).

Rv3500c (*yrbE4B*) encodes a putative ABC transporter predicted to be involved in lipid catabolism. It is in the *kstR* regulon, which contains some 74 genes involved in the utilization of diverse lipids for energy.[5] YrbE4B is predicted to be required for growth on cholesterol.[6] Rv0953c is predicted to be an F_{420}-dependent oxidoreductase and is also in the *kstR* regulon.[5] While Rv0953c is not yet characterized, F_{420}-bearing enzymes of this class are absent in humans, not well represented in prokaryotes, but present extensively in mycobacteria, including the reduced genome of *M. leprae*, providing an attractive, although non-essential, target.[7]

M. tuberculosis transcription profile following DAQA treatment.

With the aim of uncovering the DAQA MOA, we collaborated with the Clifton Barry lab of the National Institute of Allergy and Infectious Diseases at the NIH to generate a transcription profile of *M. tuberculosis* following treatment with the compound. This profile was generated

Figure 5. Transcription profile of *M. tuberculosis* following treatment with DAQA.

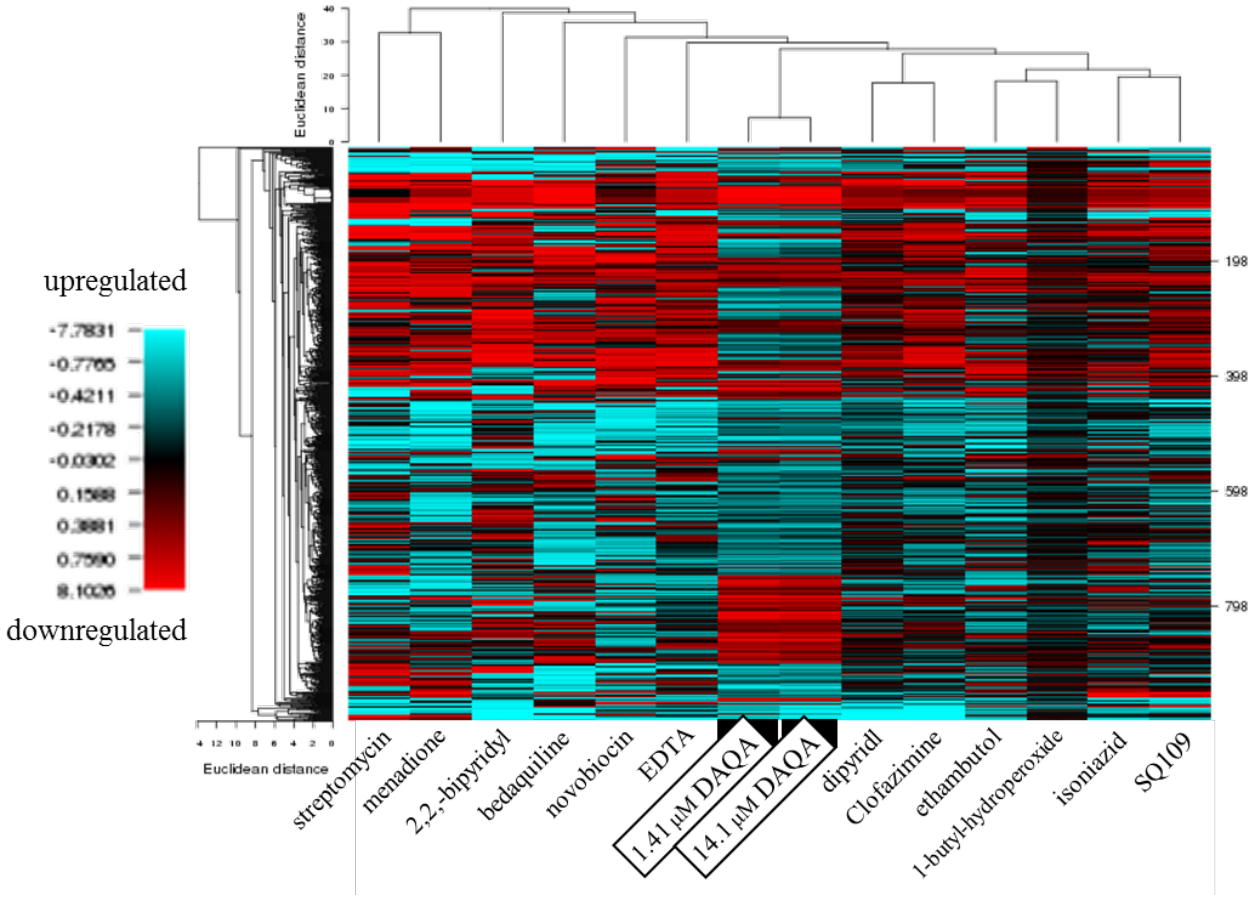

concurrently with those of well-studied TB inhibitors with the purpose of gaining insight into the DAQA MOA by comparison. The transcription pattern revealed for DAQA was consistent at the two tested concentrations, but without a close match from the known anti-TB compounds (Figure 9). Thus, no definitive conclusions about a mechanism could be inferred from these results, but some general characteristics of the DAQA mechanism could be inferred. Twenty-seven of the

thirty-two most down-regulated genes were transposases, while the most highly up-regulated genes were those coding for the peroxidase katG (Rv1908c), iron-sulfur cluster restoration, and the biosynthesis of two siderophores, mycobactin and exochelin. This combination of upregulated genes is indicative of oxidative stress while the implications of downregulated transposases are unknown.[8] In general, there was a massive oxidative stress response implicated by DAQA that was similar to that observed for known TB drugs CLF and BDQ (TMC207).[9, 10] Despite these similarities, DAQA did not have a similar effect on electron transport as CLF when tested in a separate experiment.

Clofazimine-resistant mutants are cross-resistant to DAQA.

Following observation of an oxidative stress response in the microarray study, we tested whether the mechanism was iron-dependent by screening strains of *M. tuberculosis* with DAQA first on iron-depleted GAS media, then on GAS media supplemented with a range of iron concentrations from 0 to 800 μg/L. Two clofazimine resistant mutants and a bedaquiline-resistant mutant were selected for testing along with wild type in order to further assess commonality between the DAQA mechanism and that of clofazimine or bedaquiline (Table 2). While no connection between iron concentration and activity was observed, two additional observations were made.

We first observed that *M. tuberculosis* strains were more susceptible to DAQA when they were grown on GAS media at any iron concentration than when grown on 7H12 media. This phenomenon had one exception in the bedaquiline-resistant strain rTMC207 (BK12), which has a *atpE* subunit c mutation. Why DAQA activity remains consistent between media types only in this mutant is as of yet unexplained. We subsequently investigated this difference in activities between

media types for the other strains by substituting the glycerol carbon source in GAS media with the palmitic acid carbon source from 7H12 media, but were unable to identify a significant trend.

Table 2. Effect of iron concentration and nutrient composition on anti-TB activity of DAQA.

		Media (ferric ammonium citrate conc., µg/L)				
Compound	**Mtb strain**	**7H12 (40)**	**GAS (0)**	**GAS (50)**	**GAS (200)**	**GAS (800)**
DAQA	$H_{37}Rv$	0.30	< 0.10	< 0.10	< 0.10	< 0.10
	rCLF1	3.00	0.50	0.33	0.38	0.37
	rCLF4	2.26	0.48	0.45	0.42	0.36
	rTMC207(BK12)	0.16	0.16	0.17	0.18	0.16
RMP	$H_{37}Rv$	0.03	0.04	0.05	0.06	0.03
	rCLF1	0.08	0.10	0.05	0.03	0.01
	rCLF4	0.03	0.03	0.03	0.01	0.01
	rTMC207(BK12)	0.01	0.03	0.01	0.01	0.02
INH	$H_{37}Rv$	0.19	0.15	0.15	0.15	0.14
	rCLF1	0.15	0.15	0.12	0.18	0.14
	rCLF4	0.29	0.12	0.52	0.29	0.20
	rTMC207(BK12)	0.15	0.08	0.13	0.14	0.13
PA-824	$H_{37}Rv$	0.10	0.22	0.54	0.72	0.39
	rCLF1	> 26	> 26	> 26	> 26	> 26
	rCLF4	> 26	> 26	> 26	> 26	> 26
	rTMC207(BK12)	0.10	0.14	0.38	0.42	0.29
TMC207	$H_{37}Rv$	0.73	0.86	0.83	0.85	0.65
	rCLF1	1.86	1.24	1.25	1.67	1.58
	rCLF4	1.59	1.81	1.58	1.70	1.64
	rTMC207(BK12)	5.97	3.29	3.28	3.21	3.09
CLF	$H_{37}Rv$	0.26	0.28	0.08	0.14	0.11
	rCLF1	2.00	1.95	1.19	1.97	1.81
	rCLF4	1.37	2.10	1.74	1.86	1.54
	rTMC207(BK12)	0.14	0.29	0.15	0.15	0.14

The second observation was that mutant strains rCLF1 and rCLF4, products of an unpublished spontaneous clofazimine-resistant mutant generation study in the ITR, exhibited a cross-resistance to DAQA with a nine-fold increase in MIC on all media types. This was a welcome discovery as we have yet to achieve generation of spontaneous *M. tuberculosis* $H_{37}Rv$ mutants resistant to DAQA for genome sequencing. Thus far, each attempt results in an abundance of phenotypically

resistant colonies rather than a few truly resistant strains. These rCLF mutant strains also exhibit marked cross-resistance to PA-824 and other nitroimidazoles due to mutations in F_{420} cofactor biosynthesis genes, which are involved in the pro-drug activation mechanism of these compounds, as well as cross-resistance to bedaquiline (TMC207) due to mutations in the MmpL5 efflux suppressor gene. [11, 12]

Table 3. Genes and their descriptions from DAQA-resistant strains rCLF1 and rCLF4.

Gene Name		
rCLF1	**rCLF4**	**Enzyme function**
Rv0382c	Rv0382c	orotate phosphoribosyltransferase (PyrE); pyrimidine biosynthesis
Rv0678	Rv0678	MmpL5 efflux pump transcriptional repressor
	Rv3261*	probable F_{420} biosynthesis protein (FbiA)
Rv1173*		probable FO synthase (FbiC)
Rv2932		phenolpthiocerol synthesis type-I polyketide synthase (PpsB)
Rv0552		hypothetical amidohydrolase
	Rv0050	involved in peptidoglycan biosynthesis (PonA1)
	Rv1392	probable S-adenosylmethionine synthetase (MetK)

*Rv3261 and Rv1173 are separate genes but code for enzymes in the same pathway. Rows shaded gray to illustrate mutations shared between ITR strains rCLF1 and rCLF4.

DAQA activity against *M. tuberculosis* strains with efflux regulator, pyrimidine biosynthesis, and F_{420} biosynthesis gene mutations.

This is a continuation of unsuccessful attempts to complete **Task 3 i.** The follow-up experiments were more successful. Upon discovery of the DAQA cross-resistant mutants rCLF1 and rCLF4, we compared the genomes of each strain with the aim of identifying a common mutation responsible for resistance. Of the eight total mutations between them, those shared were present in the MmpL5 efflux pump transcriptional repressor gene (Rv0678) and the orotate phosphoribotransferase gene (Rv0382c; *pyrE*) from the pyrimidine biosynthesis pathway, while

Table 4. Susceptibility of *M. tuberculosis* mutant strains to DAQA.

Strain	MIC (μg/mL) 3	PA824	CLF	RIF
'Wild type'				
$H_{37}Rv$[a]	0.19	0.10	0.11	0.04
efflux (Rv0678); pyrimidine biosynthesis (*pyrE*); F_{420} biosynthesis[a]				
rCLF1	2.23	> 26	2.04	0.05
rCLF4	1.25	> 26	1.17	0.04
MmpL5 efflux pump repressor (Rv0678)[a]				
$H_{37}Rv_{CFZ\text{-}R1}$	0.18	0.11	0.20	0.02
$H_{37}Rv_{CFZ\text{-}R2}$	0.09	0.13	0.24	0.04
pyrimidine biosynthesis[b]				
$H_{37}Rv$ (Mizrahi)	0.8			
MTBSRM1[c]	0.8			
MTBSRM2[d]	0.8			
upp::Tn[e]	0.8			
F_{420} biosynthesis[f]				
7A2 (*fbiAB*-)	0.3	>50		
5A1 (*fbiC*-)	0.2	>50		
control strains[f]				
14A1 (Rv3547-)[g]	0.3	>50		
T3 (fgd-)[g]	0.3	>50		
rRIF-BJ[h]	0.2	0.4		

[a]screened at the ITR; [b]screened in the Mizrahi lab; [c]5-flourouracil-resistant mutant; Δa74 in *upp* causing a frameshift mutation; [d]5-flourouracil-resistant mutant, nsSNP in pyrR, Asp91Asn; [e]transposon insertion in *upp* 5-flourouracil-resistant mutant; [f]screened in the Barry lab; [g]PA824-resistant controls; [h]rifampin-resistant Beijing strain.

two others were mutations in separate genes (Rv1173; *fbiC* and Rv3261; *fbiA*) within the F_{420} biosynthetic pathway (Table 3). The mutation in the Rv0678 transcription repressor allows for efflux of clofazimine and bedaquiline by the MmpL5 pump, orotate phosphoribosyltransferase (PyrE) is involved in catalyzing the synthesis of pyrimidine biosynthesis intermediate orotidine 5'-monophosphate (OMP), and F_{420} is a flavin derivative cofactor involved in numerous bacterial redox reactions.[112,12, 13] The Rv0678 repressor and *fbiA* genes are classified as non-essential by Himar1-based transposon mutagenesis but *pyrE* and *fbiC* were found to be essential.[5, 14]

We identified strains with single-mutations of each mutation shared between the rCLF mutants. These were screened in order to confirm the role of each mutation in DAQA resistance (Table 4). Our first bioassay revealed that *M. tuberculosis* Rv0678 mutant strains from the Stewart Cole lab, $H_{37}Rv_{CFZ\text{-}R1}$ and $H_{37}Rv_{CFZ\text{-}R2}$,[12] were susceptible to DAQA. This all but completely nullifies the possibility that DAQA is a substrate of the MmpL5 efflux system since rCFL4 and $H_{37}Rv_{CFZ\text{-}R1}$ share gene sequence mutations while mutations in rCLF1 and $H_{37}Rv_{CFZ\text{-}R2}$ are unique.

We also screened for inhibition of the pyrimidine biosynthesis pathway in collaboration with the Mizrahi lab at The University of Cape Town. An *M. tuberculosis* strain with anhydrotetracycline-inducible expression (*pyrE* Tet-ON) was developed according to published methods to facilitate exploration of this enzyme and it's potential as a target for anti-tuberculosis treatment.[15] Interestingly, no sensitivity was observed in the *pyrE* Tet-ON mutant when it was treated with DAQA in the absence of anhydrotetracycline. Importantly, this strain is unstable and so far, not validated for PyrE conditional expression level. These negative results were supported when 0.39 to 100 µM concentrations of uracil, a downstream product of the PyrE enzyme, were unable to rescue $H_{37}Rv$ treated with DAQA. In a previous report, the Mizrahi lab described the anti-tuberculosis activity of 5-flourouracil (5-FU) and its MOA within the pyrimidine biosynthesis salvage pathway.[15] With this in mind, we screened DAQA and 5-FU in combination against TB with the aim of identifying synergy that would suggest pyrimidine biosynthesis inhibition, but no synergy was observed between the tested 5-FU concentrations of 0.39 to 100 µM. Pyrimidine salvage pathway mutant strains, MTBSRM1 and MTBSRM2, were also screened and both were susceptible. The observed MICs in all Mizrahi lab screenings were slightly greater than the reported MIC (0.1 µg/ml) possibly due to the strain difference and/or precipitation of the

compound, which was observed in test wells containing the highest concentrations of 6.4 and 3.2 µg/ml. Together, these studies suggest that the DAQA mechanism does not involve disruption of pyrimidine biosynthesis despite the *pyrE* gene mutation presence in both of the ITR rCLF mutant strains. This left one remaining possibility.

Having nearly eliminated the shared mutations between rCLF1 and rCLF4 in Rv0678 and *pyrE* as target candidates, we then decided to explore whether mutations shared in F_{420} biosynthesis were indicative of inhibition of that pathway by DAQA. Possible additional support for F_{420} involvement was found when the gene for the putative F_{420}-dependent Rv0953c protein was a target candidate revealed in the aforementioned OE panel screening at the IDRI. Surprisingly, these final mutations were also eliminated as possible target candidates when DAQA was able to inhibit *M. tuberculosis* strains 7A2 (*fbiAB*-) and 5A1 (*fbiC*-) with the same potency as the wild type when tested through a collaboration with the Clifton Barry lab at the NIH. Additional screenings against environmental actinomycetes based on the recognition that these microbes also utilize biochemical pathways dependent on F_{420} show some promise of assisting with MOA studies but were incomplete and inconclusive regarding the role of F_{420}.

4) Key Research Accomplishments for Entire Project Period (2014 – 2016):

- Publication of G039 molecules and their biological activity in Marine Drugs[2] (Mullowney et al. *Mar Drugs*. 13: 5815-5827, 2015)

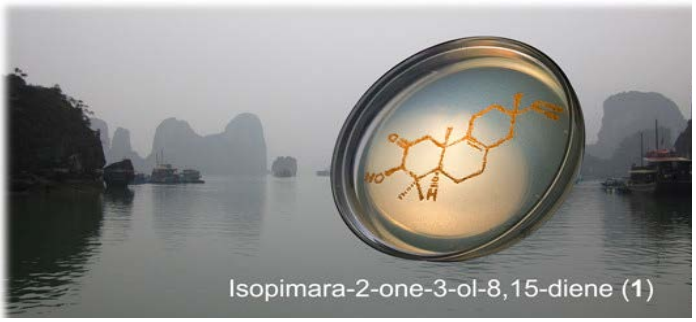

- Publication of DAQ molecules and their biological activity in ACS Infectious Diseases.[16] These are among the first freshwater actinomycete metabolites discovered to date. (Mullowney et al. *ACS Inf. Dis*. 1: 168-174, 2015); *Article featured on the cover of ACS Inf. Dis. April issue*

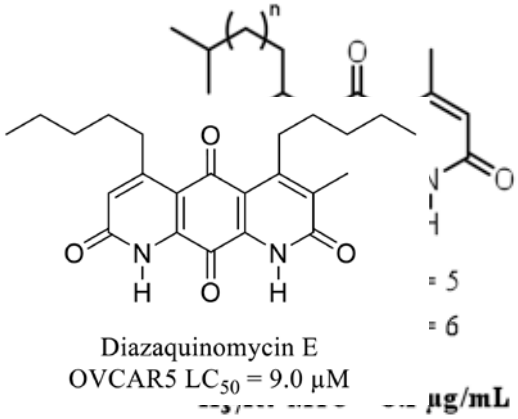

- Publication of discovery of novel diazaquinomycin analogs (strain F001) and explanation of weak cytotoxic activity (necessary for TB mechanism of action studies).[17] (Mullowney et al. *Marine Drugs* **2014**, 12, 3574)
- Optimized an efficient route for total synthesis of diazaquinomycin A
- Attempts at determining the efficacy of DAQA in mice were unsuccessful due to deaths related to the highly viscous vehicle
- DAQA exhibits potency and selectivity toward TB, while exhibiting a mechanism of action different from all known clinically available TB drugs; transcription profiling evidence suggests MoA is due to oxidative stress on the cell
- Identification and dereplication of twelve specialized metabolites from aquatic microbial strains with biological activity
- The majority of this work was the foundation of a dissertation of Dr. Michael Mullowney, who successfully defended on 11/7/16
- Work resulting from this funding received press from *NPR News*, *ACS PressPac*, *IL-IN Sea Grant*, and *UIC News*

5) Conclusion

Despite decades of research into actinomycete small molecules from terrestrial and marine environments, to the best of our knowledge identification of secondary metabolites from freshwater Actinobacteria has been virtually absent from the peer-reviewed literature. The unique

structures and activity of the diazaquinomycins provide first evidence that the Great Lakes, and more broadly freshwater environments, are a relatively unexplored resource for novel biologically active molecules.

From a *Micromonospora* sp. in Lake Michigan sediment, we isolated novel antibiotic molecules of the diazaquinomycin class. An analog, compound DAQA, displayed an *in vitro* activity profile similar or superior to clinically used TB agents and maintained potent inhibitory activity against a panel of drug-resistant TB strains. This compound displayed a selectivity profile targeted toward *M. tuberculosis*, even within the genus *Mycobacterium*. Since the 1980's, other research groups reported that members of the diazaquinomycin class exhibited weak antibacterial activity by targeting thymidylate synthase, though no reports of their anti-TB activity existed and our studies have suggested an alternate MOA in TB. Preliminary *in vitro* analysis of DAQA predicts that it will exhibit high metabolic stability, and therefore a long predicted serum half-life *in vivo*. Though DAQA was well tolerated in a dedicated five-day *in vivo* tolerance test, subsequent pharmacokinetics and efficacy experiments revealed toxicity that was suspected to be caused by the highly viscous vehicle. Additionally, DAQA was not observed above the LOQ in the PK study. This might indicate that compound exhibits poor bioavailability but the presence of the internal standard below the LOQ suggests an incompatibility of the PK methods with the poorly soluble DAQs.

Exhaustive attempts at a new DAQ total synthesis and whole cell biocatalysis methods (not discussed) were both aimed at facilitating the modification of the DAQ structure at the β-substituted position, but neither were successful. Reasons for the failed synthesis are uncertain. The biocatalysis experiment likely failed because of the limited solubility of DAQA in aqueous

media added to potential difficulty of its penetration through the lipopolysaccharide outer membrane of *E. coli*.

In the *M. tuberculosis* OE mutant screen, both Rv0953c oxidoreductase and Rv3500c transporter OE mutants exhibited a six-fold MIC increase and are predicted to be involved with lipid metabolism as part of the *kstR* regulon.[6] The fact that both mutants were resistant and contained mutations within the same regulon lends support to the potential of this pathway as a mechanism of resistance to DAQA . Importantly, the basal levels of the Rv0953c and Rv3500c genes' expression exhibited four-and two-fold increases in MIC, respectively, in the uninduced mutants. Continually overexpressed genes could lead to global metabolic pathway changes that might hinder interpretation of results such as identification of the exact site targeted in the pathway. But since these enzymes have been identified as non-essential, they are likely not targets of DAQA .[5, 14, 18] Instead, they may be involved in resistance by redox inactivation (Rv0953c) and efflux (Rv3500c) of the compound from the cell. Additionally, the oxidoreductase may protect against general ROS or DAQ-related active derivatives involved in the oxidative stress evidenced in the microarray results. Interestingly, Rv0953c and Rv3500c were not up- or down-regulated significantly in the transcription profiling study, suggesting that though some protective effect can be gained by engineering strains that upregulate these genes, *M. tuberculosis* H_{37}Rv does not innately respond to oxidative stress or DAQ treatment by this mechanism.

Though differing overall patterns in the transcription profiles suggest separate mechanisms between DAQA and other TB inhibitors, the oxidative stress response observed for the compound was similar to that from dipyridyl, menadione, and CLF.[19] Interestingly, we were able to disprove the possibility that inhibition of respiration similar to that of CLF was a part of the DAQA MOA. Because of the potential role of iron chelation in oxidative stress and a small level of resistance

observed when culturing in 7H12, [20-23] we tested the effects of iron and a palmitic acid carbon source on the activity of DAQA. We found no correlation between iron concentration in media and DAQA inhibition of *M. tuberculosis*, and were unable to identify a protective effect using the alternate carbon source.

Though we found potential MOA leads when two clofazimine-resistant strains exhibited cross-resistance to DAQA, we were unable to identify a singular target following screening of additional mutants. These experiments suggested that DAQA was not a substrate of the MmpL5 efflux system and that it did not have an effect on pyrimidine or F_{420} cofactor biosynthesis.

Also, attempts at isolating a protein target for DAQA using the DARTS assay were unsuccessful. This may be because the DAQs have a multi-faceted mechanism that may not include direct interaction with a singular protein target.

In general, the major challenges of developing DAQA as an anti-tuberculosis drug lead have been tied to the compound's limited solubility. Harsh conditions in the total synthesis have been prohibitive to derivatization aimed at improving solubility, exploring SAR, and embarking on additional MOA studies. The culmination of the aforementioned experiments saw the elimination of specific targets and pathways within a set of potential mechanisms established either through previous reports or by OE library screen and transcription profiling. More global approaches to target identification will be required in future studies to generate additional potential target leads.

Future directions.

If the DAQs are without a future as a tuberculosis therapy, additional studies into the remarkably selective mechanism still hold potential of revealing a novel target for future TB treatments. Our studies show that DAQA exhibits potency and selectivity toward TB, while exhibiting a mechanism of action different from all known clinically available TB drugs. Thus,

there is a continued focus on the characterization and eventual elucidation of the MOA in our laboratories. The most immediate goal is to generate mutant strains resistant to DAQA for full genome sequencing using the avirulent *M. tuberculosis* strain mc^27000.[24] Mutations identified to confer resistance will be prioritized as genes for potential molecular targets worthy of further investigation. The mc^27000 strain has mutations allowing for its safe use in BSL-2 containment and is a sufficient replacement for $H_{37}Rv$ with its similar susceptibility to DAQA at an MIC of 0.14 μM in the MABA.[24]

Additionally, many of the findings described in the previous chapter could be explored in greater depth. To test the specificity of the MOA of DAQA in *M. tuberculosis*, synthetic DAQ derivatives inactive in the MABA could be tested against DAQA-susceptible cancer cell lines. A similar loss of activity would suggest that the pharmacophore and possibly the MOA is shared between *M. tuberculosis* and mammalian cells, while retention of activity would suggest the opposite. Additionally, the substructure of the DAQA's central quinone coupled with results from the microarray profile suggest that extensive redox chemistry might be responsible for cell damage in *M. tuberculosis*. The selectivity of the compound opposes the assumption of such a typically promiscuous mechanism, but testing the generation of ROS by DAQA using appropriate ROS-sensitive dyes would confirm whether this suspected activity is valid.[25] Target candidates revealed from the OE mutant panel could be further investigated as well, though this would likely involve more resource-intensive molecular genetics experiments. For example, screenings of DAQA against a double Rv0953c/Rv3500c OE mutant resulting in increased resistance and tests in Rv0953c and Rv3500c transposon mutants resulting in increased susceptibility would greatly support that this lipid catabolism pathway is part of a mechanism of resistance. In a more

bioinformatic approach, discovery of the DAQ biosynthetic gene cluster may reveal closely associated resistance genes that could guide studies toward a mechanism in *M. tuberculosis*.[26]

Biocatalytic derivatization of the DAQ core to hydroxylate the β-position might be facilitated if one of the more soluble synthetic DAQ analogs was used as the substrate. Since these previously described α, O-, and N- modified derivatives tend to lack significant activity, the core of the hydroxylated product could be converted back into the more active DAQA-like structure. Once a hydroxy-DAQA was achieved, further derivatizations could be made at the reactive hydroxyl group to include photo-reactive probe moieties for target capture and pull-down.

In the absence of better-informed approaches to understanding the DAQ MOA, a systematic approach to eliminating the possibility of the canonical antibiotic mechanisms of action would be a logical step. As Walsh has eloquently described in his book *Antibiotics: Actions, Origins, Resistance*, nearly without exception, antibiotics act by one of four general modes of action: 1) inhibition of peptidoglycan synthesis in the membrane, 2) protein synthesis inhibition, 3) inhibition of DNA or RNA synthesis, or 4) inhibition of DNA/RNA precursor synthesis.[27] Studies of DAQA in these areas could identify a target or serve to further support that this class acts by a novel mechanism.

Unfortunately, attempts at determining the efficacy of DAQA in mice were unsuccessful due to deaths related to the highly viscous vehicle necessitated by the poor solubility of the compound. In the absence of a more soluble analog with retained potency, the continuation of *in vivo* evaluation for this antibiotic class is dependent on the determination of a better tolerated formulation. Use of the recently described intrapulmonary aerosol delivery method may be the ideal administration route for such an insoluble compound.[28] Following optimization of an administration method, DAQA should be tested against an acute infection model in addition to

retesting in the chronic infection model. This would allow the assessment of DAQA as a companion to bactericidal drugs *in vivo* if it is bacteriostatic. Importantly, a second attempt at quantitative pharmacokinetic data acquisition would greatly inform efficacy and additional *in vivo* experiments. These studies aim to identify a possible novel molecular target of the diazaquinomycins in TB and test the *in vivo* potential of this class as a part of further assessing their potential as anti-TB drug leads.

6) Publications, Abstracts, and Future Directions

a) Lay Press:

ACS PressPac: The ACS selected our paper in ACS Infectious Diseases to appear in their monthly press release. April 8, 2015.

Illinois-Indiana Sea Grant: Features our ACS Infectious Disease publication. March 24, 2015.

Toronto Star: Antibiotic Hunters. Murphy lab was the major feature of a piece that documented our collection trip and tuberculosis discovery efforts in Iceland. September 20, 2014.

NPR News: The Environmental Report: Murphy lab featured in an interview that describes our Great Lakes antibiotic discovery program. February 4, 2014.

UIC News Cover story: Highlights a Department of Defense grant between Drs. Murphy and Franzblau to combat the pathogen M. tuberculosis. April 17, 2013.

The Columbia Chronicle: A feature on our drug-discovery program. March 18, 2013.

Science Daily: A feature on our drug-discovery program. March 13, 2013.

b) Peer-reviewed scientific journals:

Mullowney, M. W., Ó hAinmhire, E., Tanouye, U., Burdette, J. E., Pham, V. C., Murphy, B. T. A pimarane diterpene and cytotoxic angucyclines from a marine-derived Micromonospora sp. in Vietnam's East Sea. Marine Drugs, 2015, 13, 5815.

Mullowney, M.; Hwang, C.; Newsome, A.; Wei, X.; Tanouye, U.; Wan, B.; Carlson, S.; Barranis, N.; Ó hAinmhire, E.; Chen, W.-L.; Krishnamoorthy, K.; White, J.; Blair, R.; Lee, H.; Burdette, J.; Rathod, P.; Parish, T.; Cho, S.; Franzblau, S.; Murphy, B. T. Diaza-anthracene antibiotics from a freshwater-derived actinomycete with selective antibacterial activity toward M. tuberculosis. ACS Inf. Dis. 2015, 1, 168. *Article featured on cover April 2015 issue.

Mullowney, M. W.; O'hAinmhire, E. O.; Shaikh, A.; Wei, X.; Tanouye, U.; Santarsiero, B. D.; Burdette, J. E., and Murphy, B.T. Diazaquinomycins E-G, novel diaza-anthracene analogs from a marine-derived Streptomyces sp. Mar. Drugs. 2014, 12, 3574.

c) Presentations made during the project period:

Poster presentations:

*Mullowney, M.W., Hwang, C.H., Krishnamoorthy, K., Roberts, D., Klein, L., Shaikh, A., Tanouye, U., Rathod, P., Parish, T., Cho, S., Franzblau, S., and Murphy, B.T. Diaza-anthracene antibiotics from marine and freshwater-derived actinomycete bacteria that inhibit drug-resistant *M. tuberculosis.* Marine Natural Products Gordon Conference, Ventura, CA, March 5-6, 2014.

*Mullowney, M.W., Hwang, C.H., Krishnamoorthy, K., Roberts, D., Klein, L., Shaikh, A., Tanouye, U., Rathod, P., Parish, T., Cho, S., Franzblau, S., and Murphy, B.T. Diaza-anthracene antibiotics from marine and freshwater-derived actinomycete bacteria that inhibit drug-resistant *M. tuberculosis*. Marine Natural Products Gordon-Merck Research Seminar, Ventura, CA, March 9, 2014.

*Mullowney, M.W., Hwang, C.H., Krishnamoorthy, K., Roberts, D., Klein, L., Shaikh, A., Tanouye, U., Rathod, P., Parish, T., Cho, S., Franzblau, S., and Murphy, B.T. Diaza-anthracene antibiotics from marine and freshwater-derived actinomycete bacteria that inhibit drug-resistant *M. tuberculosis.* The 52nd Annual MIKI Medicinal Chemistry Meeting in Miniature, Chicago, IL, April 12, 2014.

*Mullowney, M.W.; Hwang, C.H.; Newsome, A.; Krishnamoorthy, K.; Roberts, D.; Klein, L.; Shaikh, A.; Tanouye, U.; Rathod, P.; Parish, T.; Cho, S.; Franzblau, S.G.; and Murphy, B.T. Diaza-anthracene antibiotics from marine and freshwater-derived actinomycete bacteria that inhibit drug-resistant *M. tuberculosis.* David J. Slatkin Symposium, Chicago, IL. November 15, 2014.

*Mullowney, M.W., Ó hAinmhire, E., Tanouye, U., Wan, B., Cho S., Franzblau, S.G., Burdette, J.E., Pham, V.C., Murphy, B.T. "A novel diterpene and cytotoxic molecules from a marine-derived actinomycete in Vietnam." The 53rd Annual MIKI Medicinal Chemistry Meeting in Miniature, Lawrence, KS, April 2015.

*Mullowney, M.W., Ó hAinmhire, E., Tanouye, U., Burdette, J.E., Pham, V.C., Murphy, B.T. "A novel pimarane diterpene and cytotoxic angucyclines from a marine-derived *Micromonospora* sp. in Vietnam's East Sea." American Society of Pharmacognosy 2015 Annual Meeting, Copper Mountain, CO, July 2015.

Oral presentations:

*Mullowney, M. W. - Diaza-anthracene antibiotics that inhibit drug-resistant *Mycobacterium tuberculosis*. Joint Baxter-UIC NMR Meeting, Chicago, IL, May 21, 2014.

*Mullowney, M.W. - Natural Products Drug Discovery: Inhibitors of drug-resistant *M. tuberculosis* from aquatic actinomycetes. Invited research talk presented at the "Careers in Scientific Research" event at DePaul University, Chicago, IL, May 15, 2015.

Fitz-Henley, J. - Isolation and structure elucidation of natural product antibiotics with inhibitory activity against *Mycobacterium tuberculosis.* 1) UIC SROP Research Symposium, Chicago, IL, July 2015; 2) Illinois Summer Research Symposium, Chicago, IL, July 2015.

Murphy, B. T.– University of Illinois at Chicago – Rockford Campus, College of Pharmacy; Diaza- anthracene antibiotics that inhibit drug-resistant *Mycobacterium tuberculosis*. - 02/03/14

Murphy, B. T.– Seoul National University, Seoul, South Korea. Diaza-anthracene antibiotics from an underexplored source – freshwater-derived actinomycete bacteria – that inhibit drug-resistant *M. tuberculosis.* - 04/28/14

Murphy, B. T.– US-China Marine Biotechnology Summit, Yantai, China; "Prospecting Freshwater Sources for Drug-lead Discovery." - 08/20/14

Murphy, B. T.– David Slatkin Symposium, Chicago, IL; "Prospecting Freshwater Sources for Drug-lead Discovery." - 11/15/14

Murphy, B. T.– Perlman Symposium on Antibiotic Discovery and Development, University of Wisconsin Madison; “Prospecting Freshwater Sources for Drug-lead Discovery.” - 05/01/15

Murphy, B. T.– Andrews University, Berrien Springs, MI; “Harnessing the cultivatable microbiome in the Great Lakes to combat *Mycobacterium tuberculosis*.” - 10/05/15

7) Inventions, Patents, and Licenses

Nothing to report

8) Reportable Outcomes

i. Identification and dereplication of twelve specialized metabolites from aquatic microbial strains with biological activity.

ii. Optimized an efficient route for total synthesis of diazaquinomycin A.

iii. DAQA exhibits potency and selectivity toward TB, while exhibiting a mechanism of action different from all known clinically available TB drugs.

iv. Transcription profiling evidence suggests DAQA MoA is due to oxidative stress on the cell.

v. A total of three peer-reviewed publications, six poster presentations, and nine oral presentations at local, national, and international conferences and settings.

9) Other Achievements

i. Graduation of one student, Michael Mullowney who dedicated his dissertation work to the study of DAQA. Michael received four awards/scholarships as a result of this work.

ii. Research training of one underrepresented minority undergraduate student (Jewelle Fitz-Henley), who volunteered in the laboratory and won four university-level awards, and presented her work at a local research forum.

10) References

(1) (WHO), W.H.O., *Global Tuberculosis Report 2014.* 2014.

(2) Mullowney, M.W., O.h. E, U. Tanouye, J.E. Burdette, V.C. Pham, and B.T. Murphy, *A Pimarane Diterpene and Cytotoxic Angucyclines from a Marine-Derived Micromonospora sp. in Vietnam's East Sea.* Mar Drugs, 2015. **13**(9): p. 5815-27.

(3) Lomenick, B., R. Hao, N. Jonai, R.M. Chin, M. Aghajan, S. Warburton, J. Wang, R.P. Wu, F. Gomez, J.A. Loo, J.A. Wohlschlegel, T.M. Vondriska, J. Pelletier, H.R. Herschman, J. Clardy, C.F. Clarke, and J. Huang, *Target identification using drug affinity responsive target stability (DARTS).* Proc Natl Acad Sci U S A, 2009. **106**(51): p. 21984-21989.

(4) Pai, M.Y., B. Lomenick, H. Hwang, R. Schiestl, W. McBride, J.A. Loo, and J. Huang, *Drug affinity responsive target stability (DARTS) for small molecule target identification.* Methods Mol. Biol., 2015. **1263**: p. 287-298.

(5) Griffin, J.E., J.D. Gawronski, M.A. DeJesus, T.R. Ioerger, B.J. Akerley, and C.M. Sassetti, *High-resolution phenotypic profiling defines genes essential for mycobacterial growth and cholesterol catabolism.* PLoS Pathog, 2011. **7**(9): p. e1002251.

(6) Kendall, S.L., M. Withers, C.N. Soffair, N.J. Moreland, S. Gurcha, B. Sidders, R. Frita, A. Ten Bokum, G.S. Besra, J.S. Lott, and N.G. Stoker, *A highly conserved transcriptional repressor controls a large regulon involved in lipid degradation in Mycobacterium smegmatis and Mycobacterium tuberculosis.* Mol. Microbiol., 2007. **65**(3): p. 684-699.

(7) Selengut, J.D. and D.H. Haft, *Unexpected abundance of coenzyme F_{420}-dependent enzymes in Mycobacterium tuberculosis and other actinobacteria.* J. Bacteriol., 2010. **192**(21): p. 5788-5798.

(8) Voskuil, M., I. Bartek, K. Visconti, and G. Schoolnik, *The response of Mycobacterium tuberculosis to reactive oxygen and nitrogen species.* Frontiers in Microbiology, 2011. **2**: p. 105.

(9) Hards, K., J.R. Robson, M. Berney, L. Shaw, D. Bald, A. Koul, K. Andries, and G.M. Cook, *Bactericidal mode of action of bedaquiline.* J. Antimicrob. Chemother., 2015. **70**(7): p. 2028-2037.

(10) Yano, T., S. Kassovska-Bratinova, J.S. Teh, J. Winkler, K. Sullivan, A. Isaacs, N.M. Schechter, and H. Rubin, *Reduction of clofazimine by mycobacterial type 2 NADH:quinone oxidoreductase: a pathway for the generation of bactericidal levels of reactive oxygen species.* J Biol Chem, 2011. **286**(12): p. 10276-10287.

(11) Singh, R., U. Manjunatha, H.I.M. Boshoff, Y.H. Ha, P. Niyomrattanakit, R. Ledwidge, C.S. Dowd, I.Y. Lee, P. Kim, L. Zhang, S. Kang, T.H. Keller, J. Jiricek, and C.E. Barry, *PA-824 kills nonreplicating Mycobacterium tuberculosis by intracellular NO release.* Science, 2008. **322**(5906): p. 1392-1395.

(12) Hartkoorn, R.C., S. Uplekar, and S.T. Cole, *Cross-resistance between clofazimine and bedaquiline through upregulation of MmpL5 in Mycobacterium tuberculosis.* Antimicrobial Agents and Chemotherapy, 2014. **58**(5): p. 2979-2981.

(13) Zhang, S., J. Chen, P. Cui, W. Shi, W. Zhang, and Y. Zhang, *Identification of novel mutations associated with clofazimine resistance in Mycobacterium tuberculosis.* J. Antimicrob. Chemother., 2015. **70**(9): p. 2507-2510.

(14) Sassetti, C.M., D.H. Boyd, and E.J. Rubin, *Genes required for mycobacterial growth defined by high density mutagenesis.* Mol. Microbiol., 2003. **48**(1): p. 77-84.

(15) Singh, V., M. Brecik, R. Mukherjee, J.C. Evans, Z. Svetlikova, J. Blasko, S. Surade, J. Blackburn, D.F. Warner, K. Mikusova, and V. Mizrahi, *The complex mechanism of antimycobacterial action of 5-fluorouracil.* Chem Biol, 2015. **22**(1): p. 63-75.
(16) Mullowney, M.H., C.; Newsome, A.; Wei, X.; Tanouye, U.; Wan, B.; Carlson, S.; Barranis, N.; Ó hAinmhire, E.; Chen, W.-L.; Krishnamoorthy, K.; White, J.; Blair, R.; Lee, H.; Burdette, J.; Rathod, P.; Parish, T.; Cho, S.; Franzblau, S.; Murphy, B. T. , *Diaza-anthracene antibiotics from a freshwater-derived actinomycete with selective antibacterial activity toward M. tuberculosis.* ACS Infectious Diseases, 2015. **1**: p. 168-174.
(17) Mullowney, M.W., O.h. E, A. Shaikh, X. Wei, U. Tanouye, B.D. Santarsiero, J.E. Burdette, and B.T. Murphy, *Diazaquinomycins E-G, novel diaza-anthracene analogs from a marine-derived Streptomyces sp.* Mar Drugs, 2014. **12**(6): p. 3574-86.
(18) Lamichhane, G., M. Zignol, N.J. Blades, D.E. Geiman, A. Dougherty, J. Grosset, K.W. Broman, and W.R. Bishai, *A postgenomic method for predicting essential genes at subsaturation levels of mutagenesis: application to Mycobacterium tuberculosis.* Proc Natl Acad Sci U S A, 2003. **100**(12): p. 7213-7218.
(19) Barry, V.C., J.G. Belton, M.L. Conalty, J.M. Denneny, D.W. Edward, J.F. O'Sullivan, D. Twomey, and F. Winder, *A new series of phenazines (rimino-compounds) with high antituberculosis activity.* Nature, 1957. **179**: p. 1013-1015.
(20) Niwa, Y., T. Sakane, Y. Miyachi, and M. Ozaki, *Oxygen metabolism in phagocytes of leprotic patients: Enhanced endogenous superoxide dismutase activity and hydroxyl radical generation by clofazimine.* J Clin Microbiol, 1984. **20**(5): p. 837-842.
(21) Smith, F. and F.P. Richter, *Substituted 1,10-phenanthroline ferrous complex oxidation-reduction indicators potential determinations as a function of acid concentration.* Ind. Eng. Chem., Anal. Ed., 1944. **16**(9): p. 580-581.
(22) Kohanski, M.A., D.J. Dwyer, B. Hayete, C.A. Lawrence, and J.J. Collins, *A common mechanism of cellular death induced by bactericidal antibiotics.* Cell, 2007. **130**(5): p. 797-810.
(23) Wang, X. and X. Zhao, *Contribution of oxidative damage to antimicrobial lethality.* Antimicrobial Agents and Chemotherapy, 2009. **53**(4): p. 1395-1402.
(24) Ojha, A.K., A.D. Baughn, D. Sambandan, T. Hsu, X. Trivelli, Y. Guerardel, A. Alahari, L. Kremer, W.R. Jacobs, and G.F. Hatfull, *Growth of Mycobacterium tuberculosis biofilms containing free mycolic acids and harbouring drug-tolerant bacteria.* Mol. Microbiol., 2008. **69**: p. 164-174.
(25) Dwyer, D.J., P.A. Belenky, J.H. Yang, I.C. MacDonald, J.D. Martell, N. Takahashi, C.T.Y. Chan, M.A. Lobritz, D. Braff, E.G. Schwarz, J.D. Ye, M. Pati, M. Vercruysse, P.S. Ralifo, K.R. Allison, A.S. Khalil, A.Y. Ting, G.C. Walker, and J.J. Collins, *Antibiotics induce redox-related physiological alterations as part of their lethality.* Proc Natl Acad Sci U S A, 2014. **111**(20): p. E2100-E2109.
(26) Johnston, C.W., M.A. Skinnider, C.A. Dejong, P.N. Rees, G.M. Chen, C.G. Walker, S. French, E.D. Brown, J. Berdy, D.Y. Liu, and N.A. Magarvey, *Assembly and clustering of natural antibiotics guides target identification.* Nat. Chem. Biol., 2016. **12**(4): p. 233-239.
(27) Walsh, C., *Antibiotics: Actions, origins, resistance*. 2003, Washington, DC: ASM Press. 345.
(28) Gonzalez-Juarrero, M., L.K. Woolhiser, E. Brooks, M.A. DeGroote, and A.J. Lenaerts, *Mouse model for efficacy testing of antituberculosis agents via intrapulmonary delivery.* Antimicrobial Agents and Chemotherapy, 2012. **56**: p. 3957-3959.

ACS | Infectious Diseases

APRIL 2015
VOLUME 1
NUMBER 4
pubs.acs.org/infectious

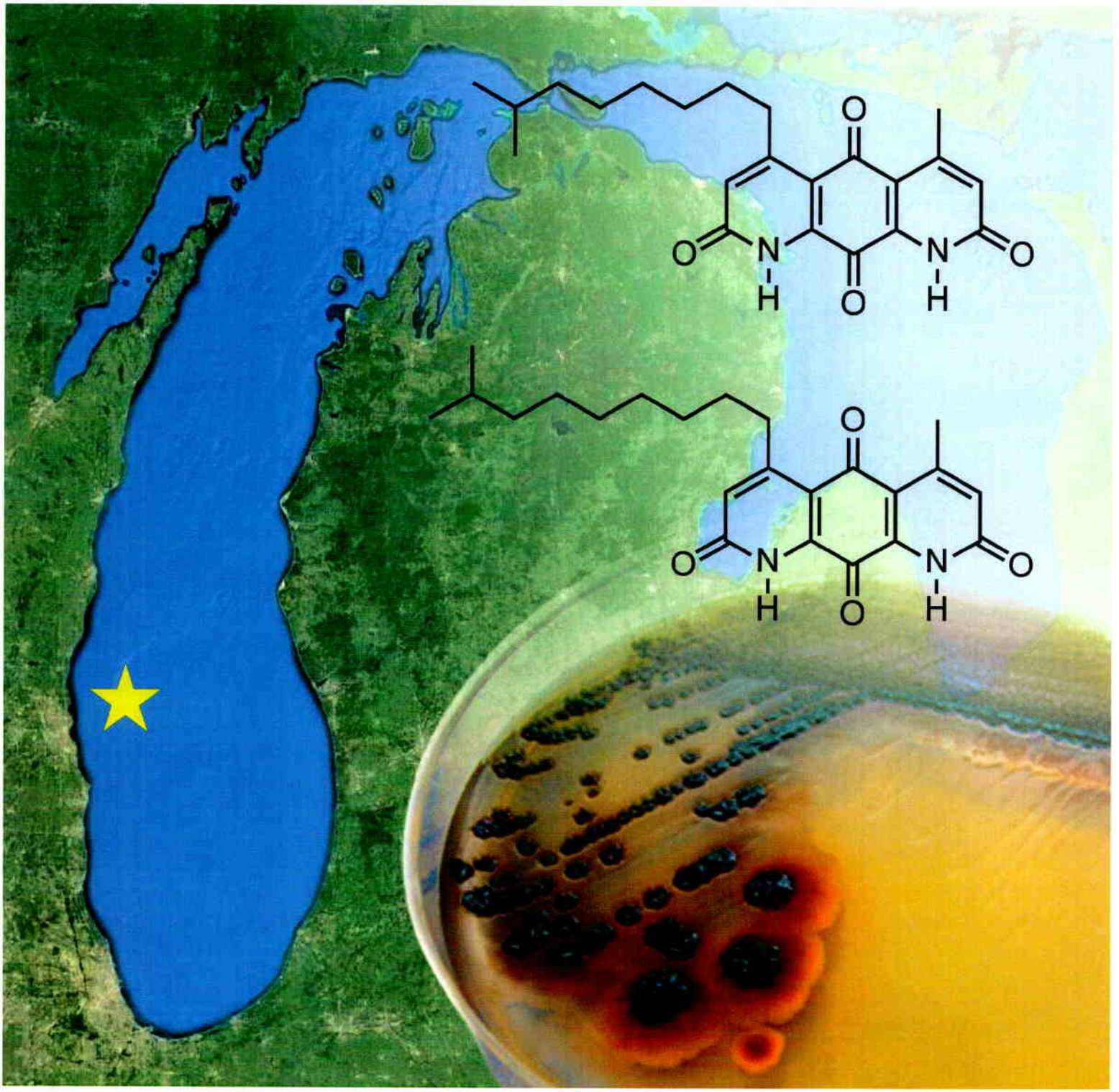

ACS Publications
Most Trusted. Most Cited. Most Read.

www.acs.org

ACS Infectious Diseases

Article

pubs.acs.org/journal/aidcbc

Diaza-anthracene Antibiotics from a Freshwater-Derived Actinomycete with Selective Antibacterial Activity toward *Mycobacterium tuberculosis*

Michael W. Mullowney,[†] Chang Hwa Hwang,[†,‡] Andrew G. Newsome,[†] Xiaomei Wei,[†] Urszula Tanouye,[†] Baojie Wan,[‡] Skylar Carlson,[†] Nanthida Joy Barranis,[†,⊥] Eoghainín Ó hAinmhire,[†,§] Wei-Lun Chen,[†] Kalyanaraman Krishnamoorthy,[∥] John White,[∥] Rachel Blair,[△] Hyunwoo Lee,[⊥] Joanna E. Burdette,[†,§] Pradipsinh K. Rathod,[∥] Tanya Parish,[△] Sanghyun Cho,[‡] Scott G. Franzblau,[†,‡] and Brian T. Murphy*[,†,§]

[†]Department of Medicinal Chemistry and Pharmacognosy, College of Pharmacy, University of Illinois at Chicago, 833 South Wood Street (MC 781), Room 539, Chicago, Illinois 60612-7231, United States

[‡]Institute for Tuberculosis Research, College of Pharmacy, University of Illinois at Chicago, 833 South Wood Street (MC 964), Room 412, Chicago, Illinois 60612-7231, United States

[§]Center for Pharmaceutical Biotechnology, College of Pharmacy, University of Illinois at Chicago, Molecular Biology Research Building, 900 South Ashland Avenue (MC 870), Room 3150, Chicago, Illinois 60607-7173, United States

[⊥]Department of Biopharmaceutical Sciences, College of Pharmacy, University of Illinois at Chicago, 833 South Wood Street (MC 865), Room 335, Chicago, Illinois 60612-7231, United States

[∥]Department of Chemistry, University of Washington, Box 351700, Seattle, Washington 98195-1700, United States

[△]TB Discovery Research, Infectious Disease Research Institute, 1616 Eastlake Avenue East, Suite 400, Seattle, Washington 98102, United States

Supporting Information

ABSTRACT: Multidrug- and extensively drug-resistant strains of *Mycobacterium tuberculosis* are resistant to first- and second-line drug regimens and resulted in 210,000 fatalities in 2013. In the current study, we screened a library of aquatic bacterial natural product fractions for their ability to inhibit this pathogen. A fraction from a Lake Michigan bacterium exhibited significant inhibitory activity, from which we characterized novel diazaquinomycins H and J. This antibiotic class displayed an in vitro activity profile similar or superior to clinically used anti-tuberculosis agents and maintained this potency against a panel of drug-resistant *M. tuberculosis* strains. Importantly, these are among the only freshwater-derived actinomycete bacterial metabolites described to date. Further in vitro profiling against a broad panel of bacteria indicated that this antibiotic class selectively targets *M. tuberculosis*. Additionally, in the case of this pathogen we present evidence counter to previous reports that claim the diazaquinomycins target thymidylate synthase in Gram-positive bacteria. Thus, we establish freshwater environments as potential sources for novel antibiotic leads and present the diazaquinomycins as potent and selective inhibitors of *M. tuberculosis*.

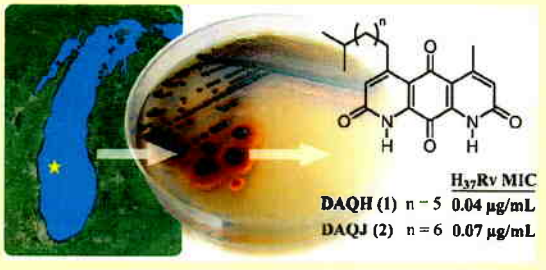

KEYWORDS: *natural products, Great Lakes, actinobacteria, antibiotic, diazaquinomycin, drug discovery*

In 2013 the World Health Organization estimated that there were 1.5 million deaths as a result of tuberculosis (TB) infection, with 9.0 million new cases reported.[1] The most significant threat to our population is multidrug- and extensively drug-resistant strains of *Mycobacterium tuberculosis* (MDR- and XDR-TB), which are resistant to first- and second-line drug regimens and resulted in 210,000 fatalities in 2013 (of 480,000 reported infections).[1−3] A major deficiency of current TB treatment is its long duration, which is necessary to eliminate a persistent subpopulation of slow-growing or nonreplicating cells. Importantly, TB is a disease that affects predominantly underprivileged populations in the developing world, and the emergence of drug-resistant forms coupled with the ease with which TB spreads between humans has solidified it as a pathogen of global concern.[4]

Natural products have been essential components of antibacterial drug discovery; they serve both as a direct source of small molecule therapies and as an inspiration for biologically active synthetic derivatives.[5] In particular, actinomycete bacteria have been an abundant source of these bioactive secondary metabolites, providing us with greater than half of the

Received: January 12, 2015
Published: March 8, 2015

DOI: 10.1021/acsinfecdis.5b00005
ACS Infect. Dis. 2015, 1, 168−174

antibiotics on the market today.[5,6] However, in previous decades extensive antibiotic screening efforts have exhausted the repertoire of unique terrestrial actinobacteria, resulting in the continuous re-isolation of known antibiotic scaffolds. As a result, researchers prospected new sources for drug lead discovery, such as the ocean. Libraries of organisms (including bacteria) and their resulting secondary metabolites were created that *were not* incorporated in the biological screening efforts of previous decades.[6,7] This investment had a considerable effect toward progress in natural product drug discovery, affording the development of several drugs from marine sources (Prialt, Yondelis, Halaven).[8−10]

The next logical step is to expand this paradigm to freshwater environments, which harbor distinct environmental selection pressures and growth conditions and to date are virtually unexplored for their capacity to afford unique actinomycete bacteria. Furthermore, despite several cultivation-independent studies aimed at characterizing lake actinomycete populations,[11] to the best of our knowledge few efforts (including one study from our laboratory) have identified secondary metabolites from freshwater-derived actinomycetes, and included in this gap is a notable absence of studies aimed specifically at generating anti-TB drug leads.[12−14] Thus, a major focus of our antibiotic discovery program is to study actinobacteria derived from the Great Lakes and other freshwater bodies. We have created an extensive library of these bacteria and their resulting secondary metabolite fractions. A preliminary in vitro growth inhibition screening of this fraction library against *M. tuberculosis* $H_{37}Rv$ led to the identification of a *Micromonospora* sp. isolated from Lake Michigan sediment, whose fraction exhibited submicromolar inhibitory activity. From this strain we isolated and characterized two novel secondary metabolites, diazaquinomycins H and J (DAQH and DAQJ), which to our knowledge are among the only freshwater-derived actinomycete metabolites described to date.[12,13] Further in vitro profiling suggested that this group of diaza-anthracene antibiotics selectively targets *M. tuberculosis* over other bacteria and is active against several forms of drug-resistant TB. Herein we present the identification and in vitro biological characterization of this unique antibiotic class.

RESULTS AND DISCUSSION

Isolation and Identification of DAQH (1) and DAQJ (2). Screening of our actinomycete secondary metabolite library against *M. tuberculosis* in the microplate Alamar Blue assay (MABA) and low-oxygen-recovery assay (LORA) led to the selection of Lake Michigan-derived strain B026 for further chemical investigation. A 28 L fermentation of B026 was performed, and following the extraction of secondary metabolites from the fermentation broth and several chromatographic steps using bioassay-guided fractionation, 0.3 mg each of **1** and **2** was purified using RP-C18 semipreparative HPLC (2.4 mL min^{-1}, gradient of 50% aqueous ACN to 100% ACN for 25 min, followed by an isocratic flow of 100% ACN for 15 min; t_R 18.6 and 22.0 min, respectively).

Detailed structure elucidation analysis for compounds **1** and **2**, including full ^1H and ^{13}C NMR assignments in addition to 2D NMR data and MS experiments, is located in the Supporting Information. Combined NMR and high-resolution IT-TOF mass spectrometry (MS) experiments of **1** established the molecular formula as $C_{22}H_{26}N_2O_4$, whereas the UV spectrum displayed a characteristic absorption profile of molecules from the diazaquinomycin class, thus helping to confirm the fused diaza-anthracene core skeleton. ^1H NMR resonances for aromatic (H3, H6) and aliphatic (H11, H12) hydrogens and their associated correlations from a heteronuclear multiple-bond correlation (HMBC) NMR experiment suggested that each lactam ring contained α-unsaturated, β-alkylated carbonyl moieties (Table S1). ^1H NMR data suggested there was a clear asymmetry to the ring system, and further exploration of the HMBC and MS data confirmed the presence of methyl and isononyl β-substituents on either lactam ring. The connectivity of each set of hydrogens in the isononyl group was determined using correlation NMR spectroscopy (COSY) and a series of one-dimensional selective total correlation spectroscopy (TOCSY) experiments (Figure 2). Therefore, the structure of **1** is as shown (Figure 1).

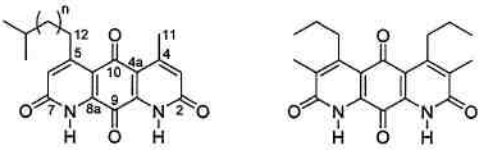

DAQH (1) n = 5 **DAQJ (2)** n = 6 **DAQA (3)**

Figure 1. Structures of diazaquinomycins H (**1**), J (**2**), and A (**3**).

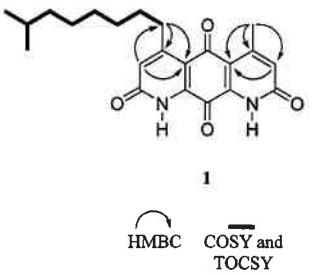

Figure 2. Key 2D NMR correlations of **1**.

Structure elucidation of DAQJ was executed in the same fashion as DAQH, using a similar series of MS and one- and two-dimensional NMR experiments to identify the molecule. A 14 Da increase in molecular weight and an extra resonance in the ^1H and ^{13}C spectra suggested an additional methylene was present in the aliphatic side chain.

In Vitro Evaluation of 1−3 in *M. tuberculosis* Whole Cell Assays. Once compounds **1** and **2** were identified, we tested their ability to inhibit replicating *M. tuberculosis* in vitro using the MABA. The MABA is a phenotypic whole cell-based microplate dilution assay that employs a fluorometric readout, relying on the correlation of resazurin dye reduction to bacterial proliferation.[15,16] Compounds **1** and **2** exhibited minimum inhibitory concentrations (MICs; defined as the lowest concentration resulting in ≥90% growth inhibition of $H_{37}Rv$ and averaged from triplicates) of 0.04 and 0.07 μg/mL, respectively. A luminescence reporter gene assay (LuxABCDE driven by hsp60) was used to confirm that the activities of **1** and **2** were not readout dependent. Further biological characterization of **1** and **2** was difficult, because a 28 L fermentation afforded only 0.3 mg of each. Fortunately, in a previous study, we isolated and identified four analogues of the diazaquinomycin antibiotic class from a marine-derived *Streptomyces* sp.[17] DAQs F and G were a coeluting isomeric mixture, but DAQA (**3**) and DAQE were purified and screened

DOI: 10.1021/acsinfecdis.5b00005
ACS Infect. Dis. 2015, 1, 168−174

Table 1. In Vitro Activity of 3 against a Drug-Resistant *M. tuberculosis* Panel

		MIC (μg/mL)					
		3	RMP[a]	INH[b]	SM[c]	KM[d]	PA824[e]
M. tuberculosis $H_{37}Rv$	MABA	0.10	<0.08	0.05	0.12	0.65	0.01
	LORA	0.72	0.85	>13.7	1.10		
Drug-resistant *M. tuberculosis* strains	rRMP	0.27	>2.00	0.02	0.27	0.92	0.03
	rINH	0.13	0.01	>2.00	0.46	0.95	0.03
	rSM	0.17	0.03	0.02	>2.00	0.95	0.11
	rKM	0.06	<0.01	0.03	1.20	>2.00	0.19
	rCS	0.14	<0.01	0.01	0.41	0.98	0.12

[a]RMP, rifampicin. [b]INH, isoniazid. [c]SM, streptomycin. [d]KM, kanamycin. [e]PA824, experimental nitroimidazole antibiotic. rRMP (ATCC 35838); rINH (ATCC 35822); rSM (ATCC 35820); rCS (cycloserine; ATCC35826); rKM (ATCC 35827).

in the MABA, exhibiting MICs of 0.1 and 0.04 μg/mL, respectively. From this strain, compound **3** was produced in relatively large amounts; thus, all further biological experiments were carried out using this molecule. Moving forward, the solubility of DAQA was an important consideration in all biological testing. DAQA exhibited a maximum room temperature concentration of 0.15 μg/mL in water in a previous study and 600 μg/mL in DMSO in the current study.[18]

We also tested **3** for its ability to inhibit nonreplicating *M. tuberculosis* in the LORA.[19] Low-oxygen adapted *M. tuberculosis* carrying the luxABCDE plasmid was exposed for 10 days to serially diluted **3** in 96-well microplates in a low-oxygen environment created with an Anoxomat commercial system. After 28 h of normoxic "recovery," activity was assessed using the ability to block recovery of the production of a luminescent signal. The MIC value of **3** was 0.72 μg/mL.

As a confirmatory approach for its anti-TB activity, the minimum bactericidal concentration (MBC_{99}; defined as the lowest concentration that reduces cfu by 99% relative to the zero time inoculum) was determined for **3** by subculture onto 7H11 agar just prior to addition of the Alamar Blue and Tween 80 for MABA MBC_{99} and reading of luminescence on day 10 from a lux reporter strain for LORA MBC_{99}. Compound **3** exhibited an MBC_{99} of 0.37 μg/mL under normoxic conditions, but did not exhibit a significant MBC_{99} under hypoxic conditions.

Cytotoxicity Evaluation of 1−3. To assess the cytotoxicity of the DAQ class, compounds **1**−**3** were tested in vitro against Vero cells (ATCC CRL-1586). They did not exhibit cytotoxicity at 28 μM, the highest testing concentration. Insufficient yields of **1** and **2** prevented further cytotoxicity screening of these compounds; however, compound **3** exhibited a range of LC_{50} values when screened against a panel of human cancerous [MDA-MB-435 (0.09 μM), MDA-MB-231 (3.6 μM), HT-29 (5.7 μM), OVCAR3 (0.48 μM), OVACR4 (4.3 μM), Kuramochi (9.4 μM)] and noncancerous cell lines [MOSE (22 μM), MOE (>28 μM)]. Further details describing these experiments can be found in the Supporting Information. Compound **3** was also tested in a previous study against ovarian cancer cell line OVCAR5 and exhibited an LC_{50} value of 8.8 μM.[17] After further investigation, we determined that the moderate cytotoxicity in this cell line was due to DNA damage via the induction of apoptosis.[17] A previous paper indicated that compound **3** and DAQC exhibited no significant inhibition when screened for antifungal activity against *Mucor miehei* and *Candida albicans*.[20] We also assessed the ability of **3** to inhibit the growth of *C. albicans* (ATCC90028), but no significant activity was exhibited when tested at the highest concentration of 10 μg/mL.

We performed a tolerance assessment of **3** in vivo. It was previously published that **3** deposited solid residues and exhibited acute toxicity when dosed at 100 mg/kg intraperitoneally,[18,21] whereas in our study the compound exhibited no qualitatively detectable ill effect and was well tolerated when dosed daily by oral gavage at 100 mg/kg for 5 days in uninfected mice. Although it is possible this difference is due to limited oral bioavailability, our Caco-2 data predict otherwise.

Antibiotic Specificity of 3 toward *M. tuberculosis*. To assess the ability of DAQA to overcome antibiotic resistance in TB and to gain potential insight into the mechanism of action for this compound class, we screened **3** against a panel of mono-drug-resistant strains using the MABA (Table 1). Compound **3** maintained potency across the panel, which suggested the absence of cross-resistance with current anti-TB agents.

To assess the specificity of **3** toward *M. tuberculosis*, we screened **3** against a panel of non-tuberculosis mycobacteria using broth microdilution with a spectrophotometric readout at A_{570} (Table 2). Interestingly, **3** exhibited selectivity toward *M. tuberculosis* and the closely related *M. bovis* BCG (MIC = 0.12 μg/mL).

In the first reports of the diazaquinomycin class, screening of **3** and its 9,10-dihydro derivative, DAQB, against a panel of bacteria revealed a relatively weak MIC of 6.25 μg/mL against three *Staphylococcus aureus* strains (FDA209P, ATCC6538P, KB199) and *Streptococcus faecium* IFO3181 while exhibiting a MIC of 1.13 μg/mL against *Micrococcus luteus*.[21,22] In the current study, we determined the MICs of **3** against a diverse panel of Gram-negative and Gram-positive pathogens.[23] Compound **3** did not exhibit significant inhibitory activity toward Gram-negative bacteria and showed weak inhibitory activity against the Gram-positive bacteria tested. The results of this and previous studies indicate that **3** possesses a narrow spectrum of activity and shows greatest inhibition toward the pathogen *M. tuberculosis*.

Caco-2 Permeability and Liver Microsome Stability of 3. Compound **3** was incubated at 1 μM for 30 min with 0.5 mg/mL of human and mouse liver microsomes and resulted in 96 and 98% of the parent compound remaining, respectively. In addition, to predict absorption via oral administration, Caco-2 bidirectional permeability was performed by incubating 5 μM **3** (with vinblastine and propranolol controls) and measuring apical and basolateral concentrations using tandem LC-MS. Compared to control compounds, **3** exhibited moderate absorption showing permeabilities of 44 nm/s with 82%

DOI: 10.1021/acsinfecdis.5b00005
ACS Infect. Dis. 2015, 1, 168−174

Table 2. Antimicrobial Spectrum of 3[a]

		MIC (μg/mL)
mycobacteria	*M. abscessus*	>7.5
	M. chelonae	>7.5
	M. marinum	>7.5
	M. kansasii	>7.5
	M. avium	3.85
	M. smegmatis	4.56
	M. bovis	0.12
G+[e]	MSSA[b]	4
	MRSA[c]	16
	E. faecalis	8
	E. faecium	8
	VRE[d]	32
	S. pyogenes	>25
	S. pneumoniae	>10
	B. thuringiensis	25
	B. cereus 14579	25
	B. cereus 10987	12.5
	B. anthracis	6.25
	B. subtilis	100
G−[f]	*A. baumannii*	128
	E. coli	128
	E. cloacae	64
	K. pneumoniae	128
	P. aeruginosa	128
	P. mirabilis	64

[a]ATCC designations are listed in the Supporting Information. [b]Methicillin-sensitive *S. aureus*. [c]Methicillin-resistant *S. aureus*. [d]Vancomycin-resistant *E. faecium*. [e]Gram-positive bacteria. [f]Gram-negative bacteria.

recovery (from apical to basolateral) and 9 nm/s with 98% recovery (from basolateral to apical) and no efflux substrate potential (0.2 efflux ratio).

Studies toward Mechanism of Action of 3. Given its mild reported antibiotic activity, observation of potency against *M. tuberculosis* provided sufficient motivation for us to further explore its biological mechanism of action. It was reported that the antibacterial activity of **3** was reversed when folate, dihydrofolate, leucovorin, and thymidine were added to the growth medium, suggesting that the target was within the folate pathway.[24] Shortly after its discovery, previous studies claimed that **3** inhibited thymidylate synthase competitively with its coenzyme 5,10-methylenetetrahydrofolate in both *E. faecium* and Ehrlich ascites carcinoma, with K_i values of 36 and 14 μM, respectively.[25] Thymidylate synthase is an attractive target as it plays a crucial role in DNA replication and repair by synthesizing de novo deoxythymidine monophosphate (dTMP) from deoxyuridine monophosphate (dUMP). *M. tuberculosis* encodes for two structurally and mechanistically unrelated thymidylate synthase enzymes (ThyA and ThyX); therefore, we attempted to determine whether either was the target of **3**.[26,27]

Using a cell-free enzyme assay, we found that **3** did not significantly inhibit the activity of purified human ThyA (HsThyA), *M. tuberculosis* ThyA (MtThyA), or MtThyX when compared to the positive control, folate analogue and known ThyA inhibitor 1843U89 (Figures S1 and S2).[28] To rule out the possibility of **3** being metabolized to a biologically active species within the cell, we performed in vitro testing against *M. tuberculosis thyA* and *thyX* overexpression mutants. We did not observe a significant differential in the MIC when **3** was screened against *M. tuberculosis thyA* and *thyX* overexpression mutants under induced (+ anhydrotetracycline) and uninduced (− anhydrotetracycline) conditions, compared to the $H_{37}Rv$ wild-type strain (Figure S3). Additionally, we observed no reversal of the antibiotic properties of **3** when the culture medium was supplemented with thymidine, indicating that there was likely no disruption in the thymidylate synthase related enzymatic processes of the folate pathway.

Despite decades of research into actinomycete small molecules from terrestrial and marine environments, to the best of our knowledge identification of secondary metabolites from freshwater actinobacteria has been virtually absent from the peer-reviewed literature. The unique structures and activity of the diazaquinomycins provide first evidence that the Great Lakes and, more broadly, freshwater environments are a relatively unexplored resource for novel biologically active molecules.

From a *Micromonospora* sp. in Lake Michigan sediment, we isolated novel antibiotic molecules of the diazaquinomycin class. An analogue, compound **3**, displayed an in vitro activity profile similar or superior to those of clinically used TB agents and maintained potent inhibitory activity against a panel of drug-resistant TB strains. This compound displayed a selectivity profile targeted toward *M. tuberculosis*, even within the genus *Mycobacterium*. Since the 1980s, other research groups have reported that members of the diazaquinomycin class exhibited weak antibacterial activity by targeting thymidylate synthase, although no reports of their anti-TB activity existed and our studies have suggested an alternate mechanism of action in *M. tuberculosis*. Preliminary in vitro analysis of **3** predicts that DAQA will exhibit high metabolic stability and, therefore, a long predicted serum half-life in vivo. Further studies are underway in our laboratories including mutant generation experiments, screening of **3** against a large overexpression library of essential *M. tuberculosis* genes, and determination of the pharmacokinetic properties of **3** in mice. These studies aim to further assess the potential of **3** as a TB drug lead and identify the molecular target of the diazaquinomycins in *M. tuberculosis*.

METHODS

Collection and Identification of Actinomycete Strain B026. Strain B026 was isolated from a sediment sample collected by PONAR at a depth of 56 m, from ca. 16.5 miles off the coast north of Milwaukee, WI, USA, in Lake Michigan (43°13′27″ N, 87°34′12″ W) on August 23, 2010. Strain B026 (GenBank accession no. KP009553) shared 100% 16S rRNA gene sequence identity with the type strain *Micromonospora maritima* strain D10-9-5 (GenBank accession no. NR109311).[29]

Isolation and Characterization of DAQH (1) and DAQJ (2) from Strain B026 Fermentation Broth. Strain B026 was grown in 28 L for 5 days at 21 °C while shaking at 220 rpm. The extracellular secondary metabolites were absorbed from the fermentation broth using Amberlite XAD-16 resin, followed by extraction with acetone and partitioning between water and ethyl acetate. The organic layer was dried under vacuum to afford 1.1 g of extract.

Using a series of bioassay-guided steps involving preparative and semipreparative normal phase (NP) and reversed phase

DOI: 10.1021/acsinfecdis.5b00005
ACS Infect. Dis. 2015, 1, 168−174

(RP) high-performance liquid chromatography (HPLC), the organic layer from the liquid–liquid partition was fractionated and purified to afford diazaquinomycin H (**1**, 0.3 mg, 0.00026% yield) and diazaquinomycin J (**2**, 0.3 mg, 0.00026% yield). See the Supporting Information for more detailed descriptions of fermentation and extraction methods for B026 and subsequent isolation and purification methods for **1** and **2**.

Diazaquinomycin H (1): red solid (0.3 mg); UV (MeOH) λ_{max} (log ε) = 278 (3.83), 301 (3.72), 357 (3.26), and a broad absorption with maximum at 472 (2.59) nm; ^{1}H NMR (900 MHz, $CDCl_3$–1% CF_3CO_2D) and ^{13}C NMR (226.2 MHz, $CDCl_3$–1% CF_3CO_2D), see Table S1; HRESI-ITTOF MS *m/z* 383.1993 $[M + H]^+$ (calcd for $C_{22}H_{27}N_2O_4$, 383.1971), *m/z* 381.1771 $[M - H]^-$ (calcd for $C_{22}H_{25}N_2O_4$, 381.1820), *m/z* 765.3778 $[2M + H]^+$ (calcd for $C_{44}H_{53}N_4O_8$, 765.3863), and *m/z* 763.3639 $[2M - H]^-$ (calcd for $C_{44}H_{51}N_4O_8$, 763.3712).

Diazaquinomycin J (2): red solid (0.3 mg); UV (MeOH) λ_{max} (log ε) = 278 (3.37), 300 (3.26), 356 (2.90), and a broad absorption with maximum at 472 (2.44) nm; ^{1}H NMR (900 MHz, $CDCl_3$–1% CF_3CO_2D) and ^{13}C NMR (226.2 MHz, $CDCl_3$–1% CF_3CO_2D), see Table S1; HRESI-ITTOF MS *m/z* 397.2162 $[M + H]^+$ (calcd for $C_{23}H_{29}N_2O_4$, 397.2127), *m/z* 395.1924 $[M - H]^-$ (calcd for $C_{23}H_{27}N_2O_4$, 395.1976), *m/z* 793.4129 $[2M + H]^+$ (calcd for $C_{46}H_{57}N_4O_8$, 793.4176), and *m/z* 791.3825 $[2M - H]^-$ (calcd for $C_{46}H_{55}N_4O_8$, 791.4025).

In Vivo Tolerance Assessment of 3. Compound **3** was prepared in a dosing vehicle of 10% polyethylene glycol 400 (PEG 400), 10% polyoxyl 35 castor oil (Kolliphor EL, BASF), and 80% oleic acid. The formulation was then administered by oral gavage at 100 mg/kg of **3** to a pair of female BALB/c mice once daily for 5 days followed by observation for qualitative indicators of toxicity (e.g., weight loss, ragged fur, huddling). Approval for animal studies was provided by the Office of Animal Care and Institutional Biosafety (OACIB) Institutional Biosafety Committee (IBC), case 12-183.

Cell-free ThyA and ThyX Enzyme Inhibition Assay. Overexpression and purification of *M. tuberculosis* ThyA and ThyX were performed as detailed in Hunter et al.[28] Human thymidylate synthase A gene (commonly referred to as TYMS) in pET17xb was transformed into BL21(DE3)pLysS. The enzyme was overexpressed in LB media supplemented with 40 μg/mL chloramphenicol and 100 μg/mL ampicillin at 37 °C until OD_{600} 0.6, when the culture was inoculated with 1 mM IPTG and incubated further at 18 °C for 18 h. Cultures were spun down, and the cell-pellet from a 1.5 L culture was lysed in 30 mL of 20 mM potassium phosphate, 500 mM NaCl, 10 mM $MgCl_2$, 0.1 mM EDTA, and 1 mM 2-mercaptoethanol at pH 7.9 on ice by sonication (5 cycles, 1 min, 90 W). The crude extract was spun down at 4 °C and 30597 RCF. A total of 27.5 mL of clarified lysate was obtained; 5.4 g of ammonium sulfate (around 35% saturation) was added in three parts and allowed to dissolve at 4 °C. The precipitate obtained was spun-down at 4 °C and 11952 RCF. Thirty milliliters of supernatant was obtained, to which 10.75 g of ammonium sulfate (approximately 80% saturation) was added slowly at 4 °C and allowed to dissolve. The precipitate obtained was again spun-down at 4 °C and 11952 RCF. It was redissolved in 15 mL of 20 mM Tris, 100 mM NaCl, 2 mM 2-mercaptoethanol, and 10% glycerol at pH 7.8, concentrated to 7 mL, and buffer exchanged into 20 mM Tris, 100 mM NaCl, 2 mM 2-mercaptoethanol, and 10% glycerol at pH 7.8. The sample was purified on a 5 mL HiTrap Q column (low-salt buffer, 20 mM Tris, 100 mM NaCl, 2 mM 2-mercaptoethanol, and 10% glycerol at pH 7.8; high-salt buffer, 20 mM Tris, 1 M NaCl, 2 mM 2-mercaptoethanol, and 10% glycerol at pH 7.8). The protein eluted out before 40% high-salt buffer. Further purification was carried out using a Hiload 16/200 Superdex 200 pg size exclusion column using 20 mM Tris, 100 mM NaCl, 2 mM 2-mercaptoethanol, and 10% glycerol at pH 7.8. HsThyA-containing fractions were pooled and buffer exchanged into 50 mM Tris, 150 mM NaCl, 2 mM TCEP, and 30% glycerol at pH 7.8 and stored at −80 °C until further use.

MtThyA (562.8 ng), MtThyX (8.4 μg), and HsThyA (638.4 ng) were pre-incubated with inhibitors (13 μM) for 15 min at room temperature in 125 mM TES, 60 mM $MgCl_2$, 2.5 mM EDTA, and 2 mM 2-mercaptoethanol at pH 7.9. The control contained DMSO without inhibitors. FAD (10.5 μM) was included in the pre-incubation in the case of MtThyX. The total reaction volume was 151 μL for MtThyA and HsThyA and 160 μL for MtThyX.

Radiolabeled dUMP solution was made by mixing 20 μL of 5′-^{3}H-dUMP and 5 μL of 10 mM dUMP in 475 μL of water. After 15 min, mTHF (67 μM for MtThyA, 5.1 μM for MtThyX, and 5.5 μM for HsThyA) and radiolabeled dUMP (5 μL) were added to 18 μL of the enzyme/inhibitor samples. NADPH at 145 μM was also added to the MtThyX samples. All samples were incubated at room temperature for 30 min. Total reaction volume in all cases was 26 μL. Reaction was stopped after 30 min by the addition of 20 μL of stop solution (1.5 N TCA, 1.1 mM nonradioactive dUMP). A volume of 200 μL of 10% charcoal (w/v) was added, and samples were incubated on ice for 15 min before being spun-down at 4 °C and 14100 RCF for 15 min. A 100 μL aliquot of the supernatant was assayed by liquid scintillation counting to determine the amount of tritium-containing water produced by the reaction.

In Vitro Screening of 3 against *M. tuberculosis thyA* and *thyX* Overexpression Mutants. Recombinant strains were constructed in which each gene (*thyA* or *thyX*) was under the control of a tetracycline inducible promoter.[30] Plasmids were transformed into *M. tuberculosis* by electroporation.[31] Recombinant and wild-type strains were grown to late log phase in roller bottles with the presence of inducer (150 ng/mL anhydrotetracycline). The MIC of compound **3** was determined by measuring bacterial growth after 5 days in the presence of the test compound and inducer.[32] Compounds were prepared as a 10-point 2-fold serial dilution in DMSO and diluted into 7H9-Tw-OADC medium in 96-well plates with a final DMSO concentration of 2%. Each plate included assay controls for background (medium/DMSO only, no bacterial cells), zero growth (2% 100 μM rifampicin), and maximum growth (DMSO only), as well as a rifampicin dose response curve. Cultures were filtered through a 5 μm filter and inoculated to a starting OD_{590} of 0.02. Plates were incubated for 5 days, and growth was measured by OD_{590}. The percent growth was calculated and fitted to the Gompertz model.[33] MIC was defined as the minimum concentration at which growth was completely inhibited and was calculated from the inflection point of the fitted curve to the lower asymptote (zero growth).

■ ASSOCIATED CONTENT

Supporting Information

The following file is available free of charge on the ACS Publications website at DOI: 10.1021/acsinfecdis.5b00005.

DOI: 10.1021/acsinfecdis.5b00005
ACS Infect. Dis. 2015, 1, 168–174

Complete NMR assignments, 1D and 2D NMR spectra, HRMS data, and UV data for **1** and **2**, in addition to bioassay methods and figures from investigations of the bioactivity and mechanism of action of **3** (PDF)

AUTHOR INFORMATION

Corresponding Author

*(B.T.M.) Phone: (312) 413-9057. Fax: (312) 413-9303. E-mail: btmurphy@uic.edu.

Notes

The authors declare no competing financial interest.

ACKNOWLEDGMENTS

We acknowledge Dr. Russel Cuhel and the crew of the RV *Neeskay* from the Great Lakes WATER Institute at the University of Wisconsin—Milwaukee for assistance in sample collection; Mark Sadek, Anam Shaikh, and Maryam Elfeki for fraction library development and preliminary bioactivity screening of strain B026; Thomas Speltz for assistance in the large-scale fermentation of strain B026; Jhewelle Fitz-Henley for assistance in determination of DAQA solubility; the University of Illinois at Chicago Research Resources Center (UIC RRC) for assistance in acquisition of mass spectra; Dr. David Lankin for assistance in acquiring ^{13}C DEPT-Q NMR and 1D TOCSY NMR data; Dr. Benjamin E. Ramirez of the University of Illinois at Chicago Center for Structural Biology for assistance in acquiring remaining NMR data; and Biotranex LLC for in vitro ADME and PK assessment. This project was funded under Department of Defense Grant W81XWH-13-1-0171 and American Cancer Society (Illinois Division) Grant 254871. In the Burdette laboratory, this research was supported by Grant PO1 CA125066 from NCI, NIH. The Rathod laboratory activities at the University of Washington were supported by NIH Grant AI099280. This project was also supported by the Office of the Director, National Institutes of Health (OD), and National Center for Complementary and Integrative Health (NCCIH) (5T32AT007533).

REFERENCES

(1) *Global Tuberculosis Report — 2014* (2014) World Health Organization, Geneva, Switzerland, www.who.int/tb.

(2) Fischbach, M. A., and Walsh, C. T. (2009) Antibiotics for emerging pathogens. *Science 325*, 1089−1093.

(3) Dorman, S. E., and Chaisson, R. E. (2007) From magic bullets back to the magic mountain: the rise of extensively drug-resistant tuberculosis. *Nat. Med. 13*, 295−298.

(4) Glaziou, P., Falzon, D., Floyd, K., and Raviglione, M. (2013) Global epidemiology of tuberculosis. *Semin. Respir. Crit. Care Med. 34*, 3−16.

(5) Newman, D. J., and Cragg, G. M. (2012) Natural products as sources of new drugs over the 30 years from 1981 to 2010. *J. Nat. Prod. 75*, 311−335.

(6) Fenical, W., and Jensen, P. R. (2006) Developing a new resource for drug discovery: marine actinomycete bacteria. *Nat. Chem. Biol. 2*, 666−673.

(7) Murphy, B. T., Maloney, K., and Fenical, W. (2011) Marine microorganisms. In *Phytochemistry and Pharmacognosy*, Eolss Publishers, Oxford, UK.

(8) Olivera, B. M., Cruz, L. J., de Santos, V., LeCheminant, G. W., Griffin, D., Zeikus, R., McIntosh, J. M., Galyean, R., Varga, J., Gray, W. R., and Rivier, J. (1987) Neuronal calcium channel antagonists. Discrimination between calcium channel subtypes using omega-conotoxin from *Conus magus* venom. *Biochemistry 26*, 2086−2090.

(9) Rinehart, K. L., Holt, T. G., Fregeau, N. L., Stroh, J. G., Keifer, P. A., Sun, F., Li, L. H., and Martin, D. G. (1990) Ecteinascidins 729, 743, 745, 759A, 759B, and 770: potent antitumor agents from the Caribbean tunicate *Ecteinascidia turbinata*. *J. Org. Chem. 55*, 4512−4515.

(10) Pettit, G. R., Herald, C. L., Boyd, M. R., Leet, J. E., Dufresne, C., Doubek, D. L., Schmidt, J. M., Cerny, R. L., Hooper, J. N., and Rützler, K. C. (1991) Isolation and structure of the cell growth inhibitory constituents from the western Pacific marine sponge *Axinella* sp. *J. Med. Chem. 34*, 3339−3340.

(11) Newton, R. J., Jones, S. E., Eiler, A., McMahon, K. D., and Bertilsson, S. (2011) A guide to the natural history of freshwater lake bacteria. *Microbiol. Mol. Biol. Rev. 75*, 14−49.

(12) Carballeira, N. M., Pagan, M., Shalabi, F., Nechev, J. T., Lahtchev, K., Ivanova, A., and Stefanov, K. (2000) Two novel iso-branched octadecenoic acids from a *Micrococcus* species. *J. Nat. Prod. 63*, 1573−1575.

(13) Carlson, S.; Tanouye, U.; Ómarsdóttir, S.; Murphy, B. T. Phylum-specific regulation of resistomycin production in a *Streptomyces* sp. via microbial coculture. *J. Nat. Prod.* 2015, DOI: 10.1021/np500767u (accessed Jan 7, 2015).

(14) Ashforth, E. J., Fu, C., Liu, X., Dai, H., Song, F., Guo, H., and Zhang, L. (2010) Bioprospecting for antituberculosis leads from microbial metabolites. *Nat. Prod. Rep. 27*, 1709−1719.

(15) Collins, L., and Franzblau, S. G. (1997) Microplate alamar blue assay versus BACTEC 460 system for high-throughput screening of compounds against *Mycobacterium tuberculosis* and *Mycobacterium avium*. *Antimicrob. Agents Chemother. 41*, 1004−1009.

(16) Franzblau, S. G., Witzig, R. S., McLaughlin, J. C., Torres, P., Madico, G., Hernandez, A., Degnan, M. T., Cook, M. B., Quenzer, V. K., Ferguson, R. M., and Gilman, R. H. (1998) Rapid, low-technology MIC determination with clinical *Mycobacterium tuberculosis* isolates by using the microplate Alamar Blue assay. *J. Clin. Microbiol. 36*, 362−366.

(17) Mullowney, M. W., Ó hAinmhire, E., Shaikh, A., Wei, X., Tanouye, U., Santarsiero, B. D., Burdette, J. E., and Murphy, B. T. (2014) Diazaquinomycins E-G, novel diaza-anthracene analogs from a marine-derived *Streptomyces* sp. *Mar. Drugs 12*, 3574−3586.

(18) Tsuzuki, K., Yokozuka, T., Murata, M., Tanaka, H., and Omura, S. (1989) Synthesis and biological activity of analogues of diazaquinomycin A, a new thymidylate synthase inhibitor. *J. Antibiot. 42*, 727−737.

(19) Cho, S. H., Warit, S., Wan, B., Hwang, C. H., Pauli, G. F., and Franzblau, S. G. (2007) Low-oxygen-recovery assay for high-throughput screening of compounds against nonreplicating *Mycobacterium tuberculosis*. *Antimicrob. Agents Chemother. 51*, 1380−1385.

(20) Maskey, R. P., Grun-Wollny, I., and Laatsch, H. (2005) Isolation and structure elucidation of diazaquinomycin C from a terrestrial *Streptomyces* sp. and confirmation of the akashin structure. *Nat. Prod. Res. 19*, 137−142.

(21) Omura, S., Iwai, Y., Hinotozawa, K., Tanaka, H., Takahashi, Y., and Nakagawa, A. (1982) OM-704 A, a new antibiotic active against gram-positive bacteria produced by *Streptomyces* sp. *J. Antibiot. 35*, 1425−1429.

(22) Omura, S., Nakagawa, A., Aoyama, H., Hinotozawa, K., and Sano, H. (1983) The structures of diazaquinomycins A and B, new antibiotic metabolites. *Tetrahedron Lett. 24*, 3643−3646.

(23) Clinical and Laboratory Standards Institute (CLSI). (2014) *Performance Standards for Antimicrobial Susceptibility Testing*, 24th Informational Supplement, CLSI Document M100-S24, CLSI, Wayne, PA, USA.

(24) Omura, S., Murata, M., Kimura, K., Matsukura, S., Nishihara, T., and Tanaka, H. (1985) Screening for new antifolates of microbial origin and a new antifolate AM-8402. *J. Antibiot. 38*, 1016−1024.

(25) Murata, M., Miyasaka, T., Tanaka, H., and Omura, S. (1985) Diazaquinomycin A, a new antifolate antibiotic, inhibits thymidylate synthase. *J. Antibiot. 38*, 1025−1033.

(26) Myllykallio, H., Lipowski, G., Leduc, D., Filee, J., Forterre, P., and Liebl, U. (2002) An alternative flavin-dependent mechanism for thymidylate synthesis. *Science 297*, 105−107.

DOI: 10.1021/acsinfecdis.5b00005
ACS Infect. Dis. 2015, 1, 168−174

(27) Chernyshev, A., Fleischmann, T., and Kohen, A. (2007) Thymidyl biosynthesis enzymes as antibiotic targets. *Appl. Microbiol. Biotechnol. 74*, 282−289.
(28) Hunter, J. H., Gujjar, R., Pang, C. K., and Rathod, P. K. (2008) Kinetics and ligand-binding preferences of *Mycobacterium tuberculosis* thymidylate synthases, ThyA and ThyX. *PLoS One 3*, No. e2237.
(29) Songsumanus, A., Tanasupawat, S., Igarashi, Y., and Kudo, T. (2013) *Micromonospora maritima* sp. nov., isolated from mangrove soil. *Int. J. Syst. Evol. Microbiol. 63*, 554−559.
(30) Galagan, J. E., Minch, K., Peterson, M., Lyubetskaya, A., Azizi, E., Sweet, L., Gomes, A., Rustad, T., Dolganov, G., Glotova, I., Abeel, T., Mahwinney, C., Kennedy, A. D., Allard, R., Brabant, W., Krueger, A., Jaini, S., Honda, B., Yu, W. H., Hickey, M. J., Zucker, J., Garay, C., Weiner, B., Sisk, P., Stolte, C., Winkler, J. K., Van de Peer, Y., Iazzetti, P., Camacho, D., Dreyfuss, J., Liu, Y., Dorhoi, A., Mollenkopf, H. J., Drogaris, P., Lamontagne, J., Zhou, Y., Piquenot, J., Park, S. T., Raman, S., Kaufmann, S. H., Mohney, R. P., Chelsky, D., Moody, D. B., Sherman, D. R., and Schoolnik, G. K. (2013) The *Mycobacterium tuberculosis* regulatory network and hypoxia. *Nature 499*, 178−183.
(31) Goude, R., and Parish, T. (2008) Electroporation of mycobacteria. *J. Vis. Exp. 15*, No. e761.
(32) Ollinger, J., Bailey, M. A., Moraski, G. C., Casey, A., Florio, S., Alling, T., Miller, M. J., and Parish, T. (2013) A dual read-out assay to evaluate the potency of compounds active against *Mycobacterium tuberculosis*. *PLoS One 8*, No. e60531.
(33) Sirgel, F. A., Wiid, I. J., and van Helden, P. D. (2009) Measuring minimum inhibitory concentrations in mycobacteria. *Methods Mol. Biol. 465*, 173−186.

■ NOTE ADDED AFTER ASAP PUBLICATION

This paper was published on the Web on March 11, 2015, with a minor text error. The concentration of the MOSE cell line in the description of cytotoxicity of compound 3 was corrected, and the paper was reposted on March 12, 2015.

DOI: 10.1021/acsinfecdis.5b00005
ACS Infect. Dis. 2015, 1, 168−174

Mar. Drugs **2014**, *12*, 3574-3586; doi:10.3390/md12063574

OPEN ACCESS

marine drugs

ISSN 1660-3397

www.mdpi.com/journal/marinedrugs

Article

Diazaquinomycins E–G, Novel Diaza-Anthracene Analogs from a Marine-Derived *Streptomyces* sp.

Michael W. Mullowney [1], Eoghainín Ó Hainmhire [1,2], Anam Shaikh [1], Xiaomei Wei [1,2], Urszula Tanouye [1,2], Bernard D. Santarsiero [1,2], Joanna E. Burdette [1,2] and Brian T. Murphy [1,2,*]

[1] Department of Medicinal Chemistry and Pharmacognosy, University of Illinois at Chicago, Chicago, IL 60612, USA; E-Mails: mmullo2@uic.edu (M.W.M.); eohain2@uic.edu (E.Ó.H.); ashaikh5@gmail.com (A.S.); xmchuic12@gmail.com (X.W.); urszula.tanouye@gmail.com (U.T.); bds@uic.edu (B.D.S.); joannab@uic.edu (J.E.B.)

[2] Center for Pharmaceutical Biotechnology, University of Illinois at Chicago, Chicago, IL 60607, USA

* Author to whom correspondence should be addressed; E-Mail: btmurphy@uic.edu; Tel.: +1-312-413-9057; Fax: +1-312-413-4034.

Received: 12 May 2014; in revised form: 25 May 2014 / Accepted: 28 May 2014 / Published: 11 June 2014

Abstract: As part of our program to identify novel secondary metabolites that target drug-resistant ovarian cancers, a screening of our aquatic-derived actinomycete fraction library against a cisplatin-resistant ovarian cancer cell line (OVCAR5) led to the isolation of novel diaza-anthracene antibiotic diazaquinomycin E (DAQE; **1**), the isomeric mixture of diazaquinomycin F (DAQF; **2**) and diazaquinomycin G (DAQG; **3**), and known analog diazaquinomycin A (DAQA; **4**). The structures of DAQF and DAQG were solved through deconvolution of X-Ray diffraction data of their corresponding co-crystal. DAQE and DAQA exhibited moderate LC_{50} values against OVCAR5 of 9.0 and 8.8 μM, respectively. At lethal concentrations of DAQA, evidence of DNA damage was observed via induction of apoptosis through cleaved-PARP. Herein, we will discuss the isolation, structure elucidation, and biological activity of these secondary metabolites.

Keywords: actinomycete; marine; *Streptomyces*; ovarian cancer; OVCAR5; diazaquinomycin

1. Introduction

Since the 1940s, natural products have proven essential as both a direct source of small molecule cancer therapies and as an inspiration for biologically active synthetic analogs of natural products; in total 131 of the 175 small molecule cancer drugs are natural products or are derived from natural products [1]. Ovarian cancer, which is the fifth leading cause of cancer death and most lethal gynecological disease in US women, would greatly benefit from new therapies [2]. New drugs are needed because all patients are treated with the same regimen of carboplatin/paclitaxel, and sadly chemoresistant disease reoccurs in most women, resulting in death [3,4].

Our program explores the capacity of actinomycete bacteria isolated from both marine and freshwater environments to produce biologically active secondary metabolites. Screening of our actinomycete secondary metabolite library against the ovarian cancer cell line OVCAR5 led to the selection of strain F001 for further chemical investigation. After several chromatographic purification steps using bioassay-guided fractionation, we isolated diazaquinomycin E (DAQE; **1**), the isomeric mixture of diazaquinomycins F and G (DAQF, **2**; DAQG, **3**), and the known analog diazaquinomycin A (DAQA; **4**). The three new compounds are mono-normethyl analogs of the diazaquinomycin structural class. DAQE and DAQA inhibited the growth of OVCAR5 cells with moderate potency (LC_{50} = 9.0 and 8.8 μM, respectively). Further biological evaluation was performed on the most abundant analog, DAQA, while we were unable to evaluate the biological activity of the isomeric mixture of DAQF and DAQG due to their low mass yield. Details of the elucidation and biological activities are described herein.

2. Results and Discussion

2.1. Structure Elucidation of DAQE, DAQF, and DAQG

Following a series of chromatographic steps, **1** (Figure 1) was obtained as red powder. The molecular formula was assigned as $C_{23}H_{28}N_2O_4$ on the basis of combined nuclear magnetic resonance (NMR) and high-resolution mass spectrometry (MS) experiments. This formula demanded 11 degrees of unsaturation. The unique chromophore of a fused diaza-anthracene ring system consistent with the diazaquinomycin structural class was observed in the UV spectrum of **1**. Analysis of the ^{1}H-NMR spectrum of **1** suggested the presence of an isolated aromatic hydrogen (δ_H 6.94, s, H-6). Integration of the H-6, H_3-11, H_2-12, H_2-17, H_3-16, and H_3-21 resonances in the ^{1}H spectrum further supported a mono-normethylated DAQ core skeleton, revealing an integration value of three for the α-substituted methyl hydrogens (δ_H 2.32, H_3-11) rather than the typical integration value of 6 for this resonance in previously reported symmetric DAQs. This mono-normethylation afforded an asymmetry to **1**.

Analysis of ^{13}C-NMR data suggested the presence of two quinone carbonyls (δ_C 180.8, C-10; 173.1, C-9), two lactam carbonyls (δ_C 163.0, C-2; 162.9, C-7), one methine alkene carbon (δ_C 127.5, C-6), seven quaternary carbons (δ_C 159.7, C-5; 154.2, C-4; 137.8, C-3; 136.5, C-8a; 134.1, C-9a; 118.0, C-4a; 117.8, C-10a), eight methylene carbons (δ_C 34.9, C-17; 32.3, C-14; 31.8, C-19; 30.7, C-12; 29.6, C-18; 28.8, C-13; 22.5, C-15; 22.5, C-20), and three methyl carbons (δ_C 14.1, C-16; 14.1, C-21; 13.0, C-11) (Table 1). Given that the molecular formula afforded 11 degrees of unsaturation and the molecule contained four carbonyls and eight quaternary alkene carbons, the remaining degrees were

satisfied by the fused ring system. Key HMBC, COSY, and 1D-TOCSY correlations are given in Figure 2. Since the molecule is asymmetric, we were able to employ proton-based spectroscopic experiments to distinguish between resonances of the β-substituted alkyl groups. Interpretation of COSY and 1D-TOCSY data defined two distinct spin systems, which were then connected to the core ring system using HMBC correlations (Figure 3 and Supplementary Figures S4–S8).

Figure 1. Structure of diazaquinomycins E (**1**), F (**2**), G (**3**), and A (**4**).

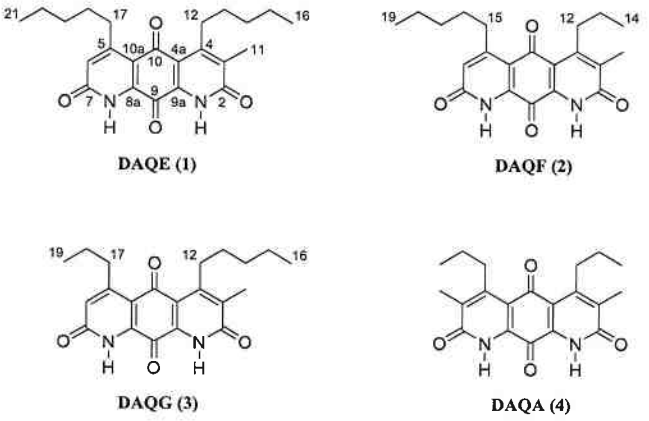

Table 1. ^{1}H and ^{13}C-NMR data ($CDCl_3$/1% CF_3CO_2D) of **1**.

Position	^{13}C [a]	^{1}H mult. (*J*, Hz) [b]
2	163.0 [c]	
3	137.8	
4	154.2	
4a	118.0	
5	159.7	
6	127.5	6.94 s
7	162.9[c]	
8a	136.5	
9	173.1	
9a	134.1	
10	180.8	
10a	117.8	
11	13.0	2.32 s
12	30.7	3.12 bt (6.4)
13	28.8	1.52 m
14	32.3	1.51 m
15	22.5	1.42 m
16	14.1	0.96 t (7.3)
17	34.9	3.11 t (7.7)
18	29.6	1.60 p (7.6)
19	31.8	1.43 m
20	22.5	1.40 m
21	14.1	0.94 t (7.3)

[a] 226.2 MHz; [b] 900 MHz; [c] resonances are interchangeable.

Figure 2. Key 2D NMR correlations of **1**.

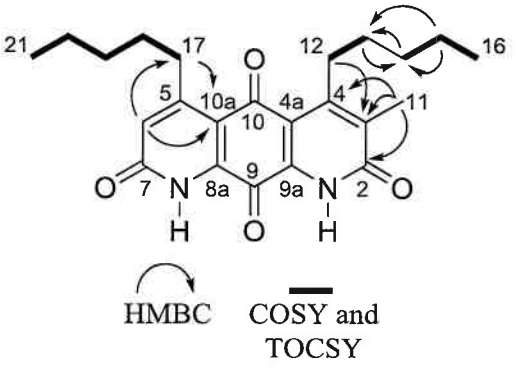

1

Figure 3. 1D TOCSY correlations of **1**. Arrows indicate irradiated resonances. (**A**) Expansion of ^{1}H-NMR spectrum (600 MHz) of **1**; (**B**) Expansion of 1D TOCSY spectrum of **1** (irradiation of 1.51 ppm); (**C**) Expansion of 1D TOCSY spectrum of **1** (irradiation of 1.62 ppm).

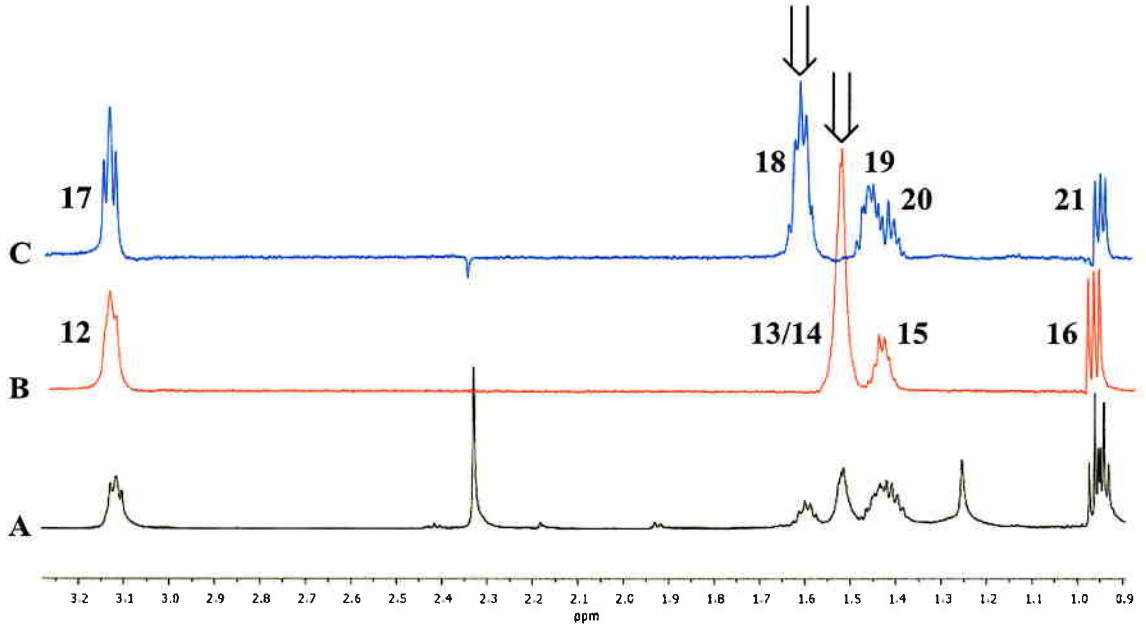

An HMBC correlation from H_2-17 to C-10a, and of H-6 to C-17 and C-10a, positioned the spin system of C-17–C-18–C-19–C-20–C-21 on the normethyl half of the diaza-anthracene core. Similarly, an HMBC correlation from H_2-12 to C-3 positioned the spin system of C-12–C-13–C-14–C-15–C-16 on the α-methylated ring of the diaza-anthracene core. Two lactam carbonyl resonances were observed in the ^{13}C DEPTQ spectrum; due to overlap it was not possible to distinguish between them in an HMBC experiment (Table 1). The remaining quinone carbons C-8a, C-9, C-9a, and C-10 were assigned based on comparison with reported values of other diazaquinomycin analogs [5,6]; our

assignments were highly consistent with reported values. Therefore, the structure of **1** was determined as shown and named diazaquinomycin E.

Following a series of chromatographic steps, the co-eluting isomeric mixture of **2** and **3** (Figure 1) was obtained as red powder. The molecular formula for the mixture of constitutional isomers was assigned as $C_{21}H_{24}N_2O_4$ on the basis of combined NMR and high-resolution MS experiments. This formula demanded 11 degrees of unsaturation. A chromophore of a fused diaza-anthracene ring system consistent with **1** was observed in the UV spectrum of the compound mixture. The diaza-anthracene core of DAQF and DAQG was determined to be mono-methylated as was previously described for **1**. This was evidenced by the presence of an aromatic hydrogen in the ^{1}H-NMR spectrum (δ_H 6.98, s, H-6 of **2** or **3**). Evidence for a second minor isomer was observed adjacent to the resonance at δ_H 6.98 (δ_H 6.95, s, H-6 of **2** or **3**) (Supplementary Information, Figures S11 and S14). Integration of the major aromatic hydrogen and the n-pentyl and n-propyl group resonances in the ^{1}H spectrum further supported a mono-normethylated DAQ core skeleton. Distinguishing separate, complete sets of ^{13}C shifts from DEPTQ and HMBC experiments was not possible due to the structural similarity and inability to separate **2** and **3**. Partial carbon shift data shared by the isomers was extracted from an HSQC experiment (Supplementary Information, Table S1). Interpretation of COSY data defined two distinct spin systems, one n-pentyl group and one n-propyl group.

To confirm the structural features observable by NMR analysis and to determine the remaining connectivity of the structures, an X-ray structure determination was attempted. The mixture of **2** and **3** co-crystallized from methanol using a slow evaporation technique. Compounds **2** and **3** occupied the same molecular site, crystallizing in the monoclinic space group $P2_1/m$ (No. 11), with a mirror plane bisecting the molecules through the central carbonyl atoms C9-O9 and C10-O10. The major isomer (**2**), present as 52.6% of the crystal, is defined with a methyl group carbon atom, C11, on atom C3 adjacent to the propyl-substituted C4 atom, and a methine group carbon atom, C6, adjacent to the pentyl-substituted C5 atom. A constitutional isomer (**3**), present as 47.4% of the crystal, is modeled with the methyl group carbon atom, C11, on atom C3 adjacent to the pentyl-substituted C4 atom, and a methine group carbon atom, C6, adjacent to the propyl-substituted C5 atom. Partially occupied water molecules are evident from the electron density maps, and near the methyl groups. The C3(methyl)-C6(H):C3(*H*)-C6(methyl) fragment occupancy was refined to a ratio of 0.704(8):0.296(8), and the C4(*n*-propyl):C4(*n*-pentyl) fragment occupancy ratio was 0.566(9):0.434(9). The molecules are packed in the crystal through hydrogen bonding with the amide hydrogen atoms and adjacent carbonyls. The intensity data was collected at experimental station 21-ID-D, Life Sciences-Collaborative Access Team (LS-CAT), at Advanced Photon Source, Argonne National Laboratory, and processed with XDS [7]. The structure was solved and refined with SHELX [8]. The final R-factor was 0.0799 for 1525 intensities greater than 2σ, and 0.0961 for all 2030 unique data. The X-ray analysis supports the proposed structures of **2** and **3** (Figure 4, Supplementary Figures S17 and S18). Therefore, **2** and **3** were determined as shown and named diazaquinomycin F and diazaquinomycin G, respectively. Crystallographic data for the structure of **2** and **3** were deposited under accession number CCDC 996646 and can be obtained free of charge from The Cambridge Crystallographic Data Centre. The ratio of **2** and **3** in the co-crystal does not necessarily reflect the weight percentage in the compound mixture, as evidenced by uneven H-6 resonances in the ^{1}H-NMR spectrum (Supplementary Figures S11 and S14).

Figure 4. Co-crystal structure of diazaquinomycin F (**2**) and diazaquinomycin G (**3**).

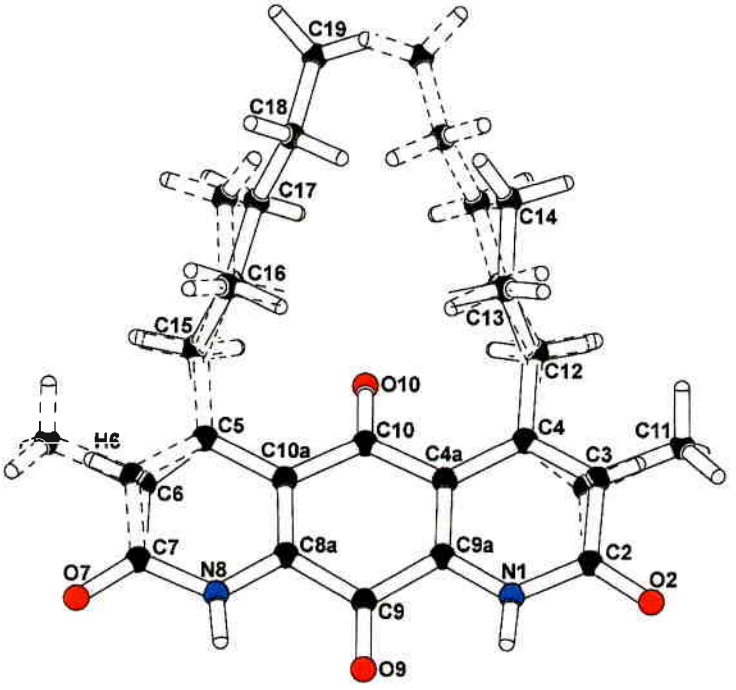

Structure numbered to emphasize DAQF occupancy in the co-crystal.

The known metabolite DAQA (**4**) was isolated and characterized based on comparison of ^{1}H-NMR and HRMS data with those appearing in literature [5,9].

2.2. DAQA (4) Induces DNA Damage, Cell Cycle Arrest, and Apoptosis through Cleaved-PARP

Compounds **1** and **4** were tested for *in vitro* cytotoxicity against the ovarian cancer cell line OVCAR5. Dose response analysis of the isolated compounds revealed an LC_{50} of 9.0 μM for **1** and 8.8 μM for **4** after treatment of cells for 96 h (Supplementary Figure S1).

Further cell-based experiments were performed on **4** due to its high yield. Western blot analysis of OVCAR5 cells treated with 17.6 μM (LC_{100}) of **4** showed increased levels of p21 (a cell cycle inhibitor) after 8 h (Figure 4). Interestingly, levels of p21 decreased after 24 h when compared to solvent control (Figure 4). Reduction of p21 protein after 24 h correlated with an increase in cleaved-PARP, an indication of apoptosis (Figure 5). The induction of cell cycle arrest, leading to apoptosis suggests significant DNA damage. To address this possibility, immunofluorescence for phospho-histone H2A.X was performed on OVCAR5 cells treated with **4** at 17.6 μM. Enhanced DNA damage, as monitored by increased phospho-histone H2A.X staining, was seen after 8 h and 24 h treatment with 17.6 μM of **4** when compared to solvent control (Figure 6a,b).

Figure 5. Compound **4** induces cell cycle arrest followed by apoptosis.

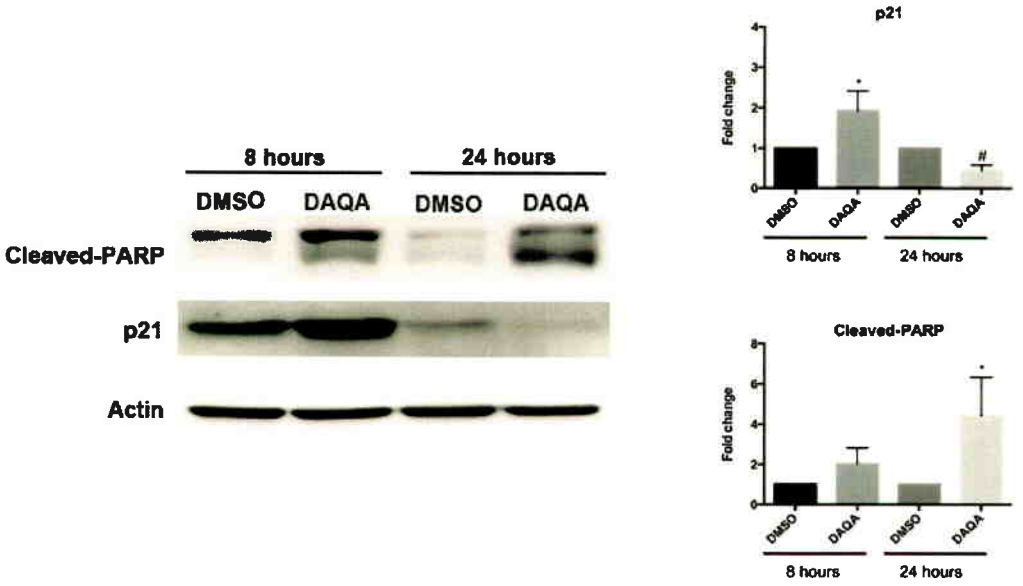

OVCAR5 cells treated with 17.6 μM of **4** showed induction of cell cycle arrest through increased p21 after 8 h, and induction of apoptosis through increased cleaved-PARP after 24 h. Densitometry of westerns was performed from three replicates. Statistical significance is donated by * for increased expression, and # for decreased expression. Student *t*-test was performed for all statistics and are represented as SEM +/−, * and # $p \leq 0.05$.

Figure 6. Compound **4** induces DNA damage in OVCAR5 cells. (**a**) H2A.X foci images taken after treatment of OVCAR5 cells with DAQA at 17.6 μM 8 h and 24 h; (**b**) Quantification of phospho-histone H2A.X foci as a fold increase over DMSO solvent control. Statistical significance is donated by * using student *t*-test. * $p \leq 0.05$.

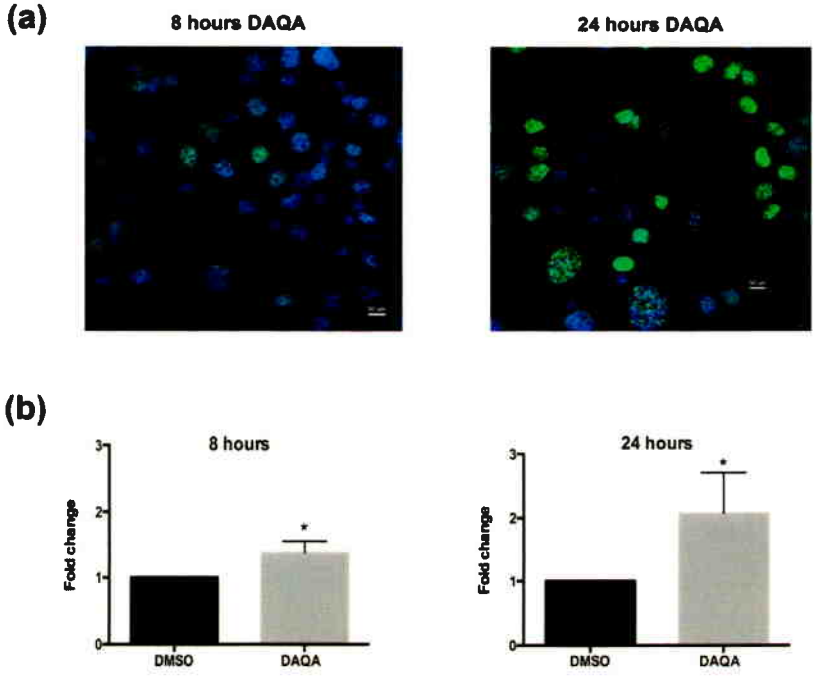

Diazaquinomycins A and B were originally isolated from a *Streptomyces* sp. after exhibiting moderate inhibitory activity against four Gram-positive bacteria (three *Staphylococcus aureus* and one *Streptococcus faecium* IFO 3181 strains) in agar-based assays [5,9]. A follow-up publication by the same group reported that DAQA exhibited cytotoxicity against Vero and Raji cell lines, while also inhibiting thymidylate synthase in Ehrlich ascites carcinoma [10]. Additional studies were carried out in order to increase the solubility and bioactivity of DAQA, and some success was achieved through modification of the C-3 and C-6 methyl groups to short chain ester and ether derivatives [11]. Nearly 15 years later, DAQC was isolated from a *Streptomyces* sp.; this report was also the first mention of DAQD, though the metabolite was only observed through (−)-ESI MS experiments and was never fully characterized [6]. The observation of an aromatic resonance in the ^{1}H spectrum (H-6) of **1** is a feature unique among existing diazaquinomycin analogs; previously reported structures of this class contain a methyl group at this position [5,6,9]. In the current study, though four secondary metabolites were isolated and characterized from strain F001, we observed ten additional diazaquinomycin analogs (based on the presence of characteristic UV spectra and MS^2 fragmentation patterns) in LCMS data of our bioactive fractions. Positive ion values ranged from *m/z* 355.1 $[M + H]^+$ to 425.2 $[M + H]^+$, and given that UV spectra remained consistent among derivatives, structural modifications likely occurred in the α-substituted methyl and β-substituted alkyl groups. Finally, **1** and **4** exhibited moderate cytotoxicity toward OVCAR5 cells by inducing apoptosis and enhancing DNA damage.

3. Experimental Section

3.1. General Experimental Procedures

UV spectra were measured on a Shimadzu Pharma Spec UV-1700 spectrophotometer (Shimadzu, Kyoto, Japan). NMR spectra were obtained on a Bruker 600 MHz DRX NMR spectrometer (Bruker, Karlsruhe, Germany) equipped with an inverse 5 mm TXI cryogenic probe with *z*-axis pfg and XWINNMR version 3.5 operating software, and a 900 (226.2) MHz Bruker AVANCE NMR spectrometer (Bruker, Karlsruhe, Germany) equipped with an inverse 5 mm TCI cryogenic probe with *z*-axis pfg and TopSpin version 1.3 operating software at the University of Illinois at Chicago Center for Structural Biology (Chicago, IL, USA). Chemical shifts (δ) are given in ppm and coupling constants (*J*) are reported in Hz. ^{1}H and ^{13}C-NMR resonances of **1** and **2** are reported in Table 1. High-resolution mass spectra were obtained on a Shimadzu ion trap-time of flight (IT-TOF) spectrometer at the University of Illinois at Chicago Research Resources Center (Chicago, IL, USA). High-performance liquid chromatography (HPLC-UV) data were obtained using a Hewlett-Packard series 1100 system controller and pumps with a Model G1315A diode array detector (DAD) (Hewlett-Packard, Palo Alto, CA, USA) equipped with a reversed-phase C_{18} column (Phenomenex Luna, 100 × 4.6 mm, 5 μm) at a flow rate of 0.5 mL·min^{-1}. Semi-preparative HPLC scale separations were performed using a Hewlett Packard Series 1050 system (Hewlett-Packard, Palo Alto, CA, USA) with a Phenomenex Luna semi-preparative C_{18} column (250 × 10 mm, 5 μm) at a flow rate of 2.4 mL·min^{-1}. Preparative HPLC scale separations were performed using a Waters LC4000 System equipped with a Phenomenex Luna preparative C_{18} column (250 × 21.2 mm, 5 μm) at a flow rate of 16 mL·min^{-1}.

3.2. Selection of Actinomycete Strain F001 for Further Investigation

We screened our library of *ca.* 2000 secondary metabolite fractions (from *ca.* 500 aquatic-derived actinomycete strains) in an *in vitro* single dose screen (20 μg/mL) against OVCAR5 and identified strain F001 as a promising bioactive lead, among other strains. Strain F001 (GenBank accession number KJ656126) shared 98% 16S rRNA gene sequence identity with the most closely related type strains *Streptomyces coacervatus* (GenBank accession number AB500703) [12], *Streptomyces hygroscopicus* subsp. *jinggangensis* (GenBank accession number NC_017765) [13], and *Streptomyces roseochromogenes* subsp. *oscitans* (GenBank accession number NZ_CM002285) [14].

3.3. Fermentation and Extraction

Strain F001 was cultured under two different media conditions. The culture that yielded **1** and **4** was grown in 44 × 1 L portions in Fernbach flasks containing high nutrient A1 medium (filtered ocean water, 10 g starch, 4 g yeast, 2 g peptone, 1 g calcium carbonate, 100 mg potassium bromide, and 40 mg iron sulfate) for 5 days at 21 °C while shaking at 220 rpm. The culture that yielded **2** and **3** was grown in 5 × 1 L portions in Fernbach flasks containing high nutrient CGS medium (filtered ocean water, 4 g casamino acids, 10 mL glycerol, and 5 g soy peptone) for 5 days at 21 °C while shaking at 220 rpm. Extraction methods for each growth condition were the same. Sterilized Amberlite XAD-16 resin (15 $g \cdot L^{-1}$) was added to each flask to absorb the extracellular secondary metabolites. The culture medium and resin were shaken for 8 h and filtered using cheesecloth to remove the resin. The resin, cell mass, and cheesecloth were extracted with acetone overnight, concentrated under vacuum, and partitioned between water and ethyl acetate. The organic layer of the A1 fermentation was dried under vacuum to afford 6.3 g of extract. The organic layer of the CGS fermentation was dried under vacuum to afford 1.1 g of extract.

3.4. Isolation and Characterization of Diazaquinomycins E (1), F (2), and G (3)

DAQE was isolated from the fermentation broth (A1 media) of strain F001. The organic layer from the liquid-liquid partition was fractionated using silica gel flash column chromatography (100 g of silica) eluting with an isocratic 95% chloroform ($CHCl_3$):5% methanol (MeOH) solvent system to afford eight fractions. Using bioassay-guided fractionation, it was determined that fractions 2 and 3 contained the bioactive constituents, thus they were combined and separated using RP-C_{18} preparative HPLC (16 $mL \cdot min^{-1}$, gradient of 50% aqueous acetonitrile (ACN) to 100% ACN for 20 min, followed by an isocratic flow of 100% ACN for 10 min) to afford nine fractions. Fraction 8 (t_R 17.2 min, 14 mg) was separated using RP-C_{18} semi-preparative HPLC (2.4 $mL \cdot min^{-1}$, gradient of 50% aqueous ACN to 100% ACN for 25 min, followed by an isocratic flow of 100% ACN for 15 min) to afford diazaquinomycin E (**1**, t_R 22.1 min, 0.9 mg, 0.014% yield).

DAQF and DAQG were isolated from the fermentation broth (CGS media) of strain F001. The organic layer from the liquid-liquid partition of the culture extract was fractionated using silica gel flash column chromatography (100 g of silica) eluting with an isocratic 95% $CHCl_3$:5% MeOH solvent system to afford eight fractions. Using bioassay-guided fractionation, it was determined that fraction 8 contained the bioactive constituents, thus, it was separated using normal phase silica gel

(NP-Si) semi-preparative HPLC (2.0 mL·min^{-1}, gradient of 99% $CHCl_3$:1% MeOH to 90% $CHCl_3$:10% MeOH for 10 min, followed by an isocratic flow of 90% $CHCl_3$:10% MeOH for 15 min) to afford 7 fractions. Fraction 4 (t_R 18.1 min, 2.2 mg) was separated using NP-Si semi-preparative HPLC (2.0 mL·min^{-1}, gradient of 99% $CHCl_3$:1% MeOH to 90% $CHCl_3$:10% MeOH for 10 min, followed by an isocratic flow of 90% $CHCl_3$:10% MeOH for 10 min) to afford 7 fractions. Fraction 5 (t_R 19.3 min, 0.4 mg) was separated using NP-Si semi-preparative HPLC (2.0 mL·min^{-1}, gradient of 99% $CHCl_3$:1% MeOH to 90% $CHCl_3$:10% MeOH for 10 min, followed by an isocratic flow of 90% $CHCl_3$:10% MeOH for 10 min) to afford the co-eluting isomeric mixture of **2** and **3** (t_R 19.3 min, 0.28 mg, 0.025% yield).

Diazaquinomycin E (1): Red solid (0.9 mg). UV (MeOH) λ_{max} (log ε) = 282.5 (3.90), 362.5 (3.24), and a broad peak with maximum at 486.0 (2.56) nm. ^{1}H-NMR (900 MHz, $CDCl_3$–1% CF_3CO_2D) and ^{13}C-NMR (226.2 MHz, $CDCl_3$–1% CF_3CO_2D), see Table 1. HRESI-ITTOF MS *m/z* 397.2198 $[M + H]^+$ (calcd. for $C_{23}H_{29}N_2O_4$: 397.2127), *m/z* 395.1943 $[M - H]^-$ (calcd. for $C_{23}H_{27}N_2O_4$: 395.1971), *m/z* 419.1997 $[M + Na]^+$ (calcd. for $C_{23}H_{28}N_2O_4Na$: 419.1947), *m/z* 793.4211 $[2M + H]^+$ (calcd. for $C_{46}H_{57}N_4O_8$: 793.4176), and *m/z* 815.3997 $[2M + Na]^+$ (calcd. for $C_{46}H_{56}N_4O_8Na$: 815.3996).

Diazaquinomycin F (2) and diazaquinomycin G (3): Red solid (0.28 mg). For UV, partial NMR, and HRMS data, see Supplementary Information (Table S1; Figures S11–S16).

3.5. OVCAR5 Cytotoxicity Assay

OVCAR5 cells were cultured in minimum essential media (Life Technologies, 11090-081, Carlsbad, CA, USA) and supplemented with 10% fetal bovine serum (Life Technologies, 16000-044) 1% L-glutamine (Life Technologies, 25030-081), 1% nonessential amino acids (Life Technologies, 11140-050), 1% sodium pyruvate (Life Technologies, 11360-050) and 1% penicillin/streptomycin (Life Technologies, 15140-122). OVCAR5 cells (5000/well) were plated in a 96 well plate one day prior to treatment. The next day, cells were treated with varying doses of the given compound in regular culture media. The doses tested were 10.0 μg/mL, 5.00 μg/mL, 2.50 μg/mL, 1.25 μg/mL, 0.625 μg/mL, 0.313 μg/mL, 0.156 μg/mL, and 0.0781 μg/mL. Doses higher than 10.0 μg/mL could not be tested due to compound insolubility in DMSO. Test plates were incubated at 37 °C with 5% CO_2 for 96 h. After 96 h, media was removed from the cells and washed with cold PBS. Cells were permanently fixed to the culture plate using 5% trichloroactetic acid (TCA). A sulforhodamine B (SRB) assay was performed as previously reported [15]. Percent survival was calculated by comparing samples treated with **1** or **4**, and samples treated with the relevant volume of DMSO solvent control. Prism 6 GraphPad was used to graph the results and determine the LC_{50} in μM concentrations.

3.6. Western Blot Analysis

Cells were plated at a density of 50,000 cells in a 6 well plate one day before treatment. Cells were treated with 17.6 μM **4** for 8 h and 24 h. DMSO was used as a solvent control. Western blot gels were run as previously described [16]. An amount of 30 μg of cell lysate was run for each sample. p21 (#9247) and cleaved-PARP (#9541) from Cell Signaling were used to probe protein membranes at concentrations of 1:1000 in 5% milk/TBS-T. Actin (Sigma-Aldrich, St. Louis, MO, USA) was used as

a loading control at a concentration of 1:1000. Anti-rabbit HRP-linked antibody (cell signaling) was used for all blots at 1:1000. Densitometry was performed using ImageJ software. All samples were performed in triplicate.

3.7. Immunofluorescence

Cells were plated at a density of 25,000 cells in a chamber slide (Millipore, PEZGS0816, Billerica, MA, USA) one day before treatment. After one day, cells were treated with 17.6 μM of **4** for 8 h and 24 h. After the treatment, cells were washed with 1X cold PBS and fixed with 4% paraformaldehyde, and permeabilized with 0.2% Triton-X100 in PBS for 10 min. Cells were then washed twice with 1× PBS and blocked with 10% goat serum in PBS. Phospho-histone H2A.X (Cell Signaling, #9178, Beverly, MA, USA) was incubated on the cells for 1 h at room temperature in 10% goat serum/PBS at a concentration of 1/100. After two PBS washes, cells were incubated with anti-rabbit AlexaFluor 488 (Life Technologies, Carlsbad, CA, USA) for 30 min at room temperature and mounted using Vectashield Mounting Medium with DAPI (Vector Laboratories, Burlingame, CA, USA). Images were taken on a Nikon E600 Microscope with a DS-Ri1 Digital Camera and NIS Elements Software (Nikon instruments, Melville, NY, USA). ImageJ software was used to count cells. The number of DAPI positive cells that were also positive for phosphor-histone H2A.X were expressed as a percentage of total DAPI stained cells. Only cells with defined foci were counted as positive. At least three random fields from three independent experiments were counted.

4. Conclusions

Three new diaza-anthracene analogs were identified, diazaquinomycin E (**1**), F (**2**), and G (**3**) from the culture broth of a marine-derived *Streptomyces* sp. DAQE and its known analog DAQA exhibited moderate cytotoxicity toward OVCAR5 cells (LC_{50} of 9.0 and 8.8 μM, respectively). At lethal concentrations of DAQA, evidence of DNA damage was seen with induction of apoptosis through cleaved-PARP. Among existing diazaquinomycins, **1–3** are the first reported members of the class to exhibit a variation in the diaza-anthracene core skeleton.

Acknowledgments

The authors would like to acknowledge Mark Sadek, Skylar Carlson, and Maryam Elfeki for fraction library development and preliminary bioactivity screening of strain F001, the University of Illinois at Chicago Research Resources Center (UIC RRC) for assistance in acquisition of mass spectra, David Lankin for assistance in acquiring ^{13}C DEPT-Q NMR data, and Benjamin E. Ramirez of the University of Illinois at Chicago Center for Structural Biology for assistance in acquiring remaining NMR data.

This project was funded under Department of Defense grant #W81XWH-13-1-0171 and American Cancer Society (Illinois Division) grant #254871. This project was also made possible by Grant Number T32AT007533 from the National Center for Complementary and Alternative Medicines (NCCAM) and the Office of Dietary Supplements (ODS). Its contents are solely the responsibility of the authors and do not necessarily represent the official views of the NCCAM, ODS, or the National

Institutes of Health. Supersedes NoA issued on 12/19/2012. Use of the Advanced Photon Source, an Office of Science User Facility operated for the U.S. Department of Energy (DOE) Office of Science by Argonne National Laboratory, was supported by the U.S. DOE under Contract No. DE-AC02-06CH11357. Use of the LS-CAT Sector 21 was supported by the Michigan Economic Development Corporation and the Michigan Technology Tri-Corridor (Grant 085P1000817).

Author Contributions

Conceived and designed the experiments: MWM, EÓH, BDS, JB, BTM. Performed the experiments: MWM, EÓH, AS, XW, UT, BDS, JB, BTM. Analyzed the data: MWM, EÓH, AS, XW, BDS, JB, BTM. Wrote the paper: MWM, EÓH, BDS, JB, BTM.

Conflicts of Interest

The authors declare no conflict of interest.

References

1. Newman, D.J.; Cragg, G.M. Natural products as sources of new drugs over the 30 years from 1981 to 2010. *J. Nat. Prod.* **2012**, *75*, 311–335.
2. Siegel, R.; Ma, J.; Zou, Z.; Jemal, A. Cancer statistics, 2014. *CA Cancer J. Clin.* **2014**, *64*, 9–29.
3. Harries, M.; Gore, M. Part I: Chemotherapy for epithelial ovarian cancer-treatment at first diagnosis. *Lancet Oncol.* **2002**, *3*, 529–536.
4. Harries, M.; Gore, M. Part II: Chemotherapy for epithelial ovarian cancer-treatment of recurrent disease. *Lancet Oncol.* **2002**, *3*, 537–545.
5. Omura, S.; Nakagawa, A.; Aoyama, H.; Hinotozawa, K.; Sano, H. The structures of diazaquinomycins A and B, new antibiotic metabolites. *Tetrahedron Lett.* **1983**, *24*, 3643–3646.
6. Maskey, R.P.; Grun-Wollny, I.; Laatsch, H. Isolation and structure elucidation of diazaquinomycin C from a terrestrial *Streptomyces* sp. and confirmation of the akashin structure. *Nat. Prod. Res.* **2005**, *19*, 137–142.
7. Kabsch, W. XDS. *Acta Crystallogr.* **2010**, *66*, 125–132.
8. Sheldrick, G.M. A short history of SHELX. *Acta Crystallogr.* **2008**, *64*, 112–122.
9. Omura, S.; Iwai, Y.; Hinotozawa, K.; Tanaka, H.; Takahashi, Y.; Nakagawa, A. OM-704 A, A new antibiotic active against gram-positive bacteria produced by *Streptomyces* sp. *J. Antibiot.* **1982**, *35*, 1425–1429.
10. Murata, M.; Miyasaka, T.; Tanaka, H.; Omura, S. Diazaquinomycin A, a new antifolate antibiotic, inhibits thymidylate synthase. *J. Antibiot.* **1985**, *38*, 1025–1033.
11. Tsuzuki, K.; Yokozuka, T.; Murata, M.; Tanaka, H.; Omura, S. Synthesis and biological activity of analogues of diazaquinomycin A, a new thymidylate synthase inhibitor. *J. Anitbiot.* **1989**, *42*, 727–737.
12. Shibazaki, A.; Omoto, Y.; Kudo, T.; Yaguchi, T.; Saito, A.; Ando, A.; Mikami, Y.; Gonoi, T. *Streptomyces coacervatus* sp. nov., isolated from the intestinal tract of *Armadillidium vulgare*. *Int. J. Syst. Evol. Microbiol.* **2011**, *61*, 1073–1077.

13. Wu, H.; Qu, S.; Lu, C.; Zheng, H.; Zhou, X.; Bai, L.; Deng, Z. Genomic and transcriptomic insights into the thermo-regulated biosynthesis of validamycin in *Streptomyces hygroscopicus* 5008. *BMC Genomics* **2012**, *13*, 337:1–337:14.
14. Ruckert, C.; Kalinowski, J.; Heide, L.; Apel, A.K. Draft genome sequence of *Streptomyces roseochromogenes* subsp. oscitans DS 12.976, producer of the aminocoumarin antibiotic clorobiocin. *Genome Announc.* **2014**, *2*, e01147–e011413.
15. Vichai, V.; Kirtikara, K. Sulforhodamine B colorimetric assay for cytotoxicity screening. *Nat. Protoc.* **2006**, *1*, 1112–1116.
16. Ó Hainmhire, E.; Quartuccio, S.M.; Cheng, W.; Ahmed, R.A.; King, S.M.; Burdette, J.E. Mutation or Loss of p53 Differentially Modifies TGFbeta Action in Ovarian Cancer. *PLoS One* **2014**, *9*, e89553.

Mar. Drugs **2015**, *13*, 5815-5827; doi:10.3390/md13095815

OPEN ACCESS

marine drugs

ISSN 1660-3397

www.mdpi.com/journal/marinedrugs

Article

A Pimarane Diterpene and Cytotoxic Angucyclines from a Marine-Derived *Micromonospora* sp. in Vietnam's East Sea

Michael W. Mullowney [1], Eoghainín Ó hAinmhire [1,2], Urszula Tanouye [1], Joanna E. Burdette [1,2], Van Cuong Pham [3] and Brian T. Murphy [1,2,*]

[1] Department of Medicinal Chemistry and Pharmacognosy, College of Pharmacy, University of Illinois at Chicago, 833 South Wood Street (MC 781), Room 539, Chicago, IL 60612-7231, USA; E-Mails: mmullo2@uic.edu (M.W.M); eohain2@uic.edu (E.Ó.); urszula.tanouye@gmail.com (U.T.); joannab@uic.edu (J.E.B.)

[2] Center for Biomolecular Sciences, College of Pharmacy, University of Illinois at Chicago, Molecular Biology Research Building, 900 South Ashland Avenue (MC 870), Room 3150, Chicago, IL 60607-7173, USA

[3] Institute of Marine Biochemistry, Vietnam Academy of Science and Technology, 18 Hoàng Quốc Việt, Cầu Giấy, Hà Nội 10000, Vietnam; E-Mail: phamvc@yahoo.com

* Author to whom correspondence should be addressed; E-Mail: btmurphy@uic.edu; Tel.: +1-312-413-9057; Fax: +1-312-413-4034.

Academic Editor: Anake Kijjoa

Received: 4 August 2015 / Accepted: 8 September 2015 / Published: 15 September 2015

Abstract: A screening of our actinomycete fraction library against the NCI-60 SKOV3 human tumor cell line led to the isolation of isopimara-2-one-3-ol-8,15-diene (**1**), lagumycin B (**2**), dehydrorabelomycin (**3**), phenanthroviridone (**4**), and WS-5995 A (**5**). These secondary metabolites were produced by a *Micromonospora* sp. isolated from sediment collected off the Cát Bà peninsula in the East Sea of Vietnam. Compound **1** is a novel $\Delta^{8,9}$-pimarane diterpene, representing one of approximately 20 actinomycete-produced diterpenes reported to date, while compound **2** is an angucycline antibiotic that has yet to receive formal characterization. The structures of **1** and **2** were elucidated by combined NMR and MS analysis and the absolute configuration of **1** was assigned by analysis of NOESY NMR and CD spectroscopic data. Compounds **2**–**5** exhibited varying degrees of cytotoxicity against a panel of cancerous and non-cancerous cell lines. Overall, this study highlights our collaborative efforts to discover novel biologically active molecules from the large, underexplored, and biodiversity-rich waters of Vietnam's East Sea.

Keywords: actinomycete; marine; *Micromonospora*; ovarian cancer; Vietnam; diterpene

1. Introduction

Natural products and their synthetic derivatives are essential toward the discovery of drugs, accounting for greater than 74% of marketed small molecule therapies [1,2]. In particular, actinomycete bacteria have provided us with an abundance of bioactive compounds, including more than half of marketed antibiotics and many clinically useful anticancer drugs [2]. Of the different classes of molecules produced by actinomycetes, the terpenes are a structurally diverse group of natural products with approximately 60,000 members. A recent study unveiled that the capacity of actinomycetes to produce diterpenes has been significantly underestimated, where 25 of 100 randomly selected strains were identified as potential diterpene producers [3]. Despite this, only an estimated twenty diterpenes of actinomycete origin have been reported to date [4]. This is an exceedingly scarce fraction of the nearly 12,000 diterpenes described in the peer-reviewed literature, which are predominantly plant- and fungal-derived. In the current study, we report the rare isolation of a diterpene from an actinomycete strain.

Our program explores the potential of marine and fresh water-derived actinomycete secondary metabolites to serve as antibiotic and anticancer drug leads [5,6]. As part of this program, the University of Illinois at Chicago has partnered with the Vietnam Academy of Science and Technology to explore the potential of Vietnam's East Sea to provide such leads. The East Sea in Vietnam covers an area of approximately three-million km^2 and traces 3000 km of coastline. This stretch is comprised of a multitude of microenvironments covering depths from 200 m to 5000 m. The marine biodiversity within the East Sea is considered to be some of the most extensive in the world, yet it remains poorly understood and explored. In the current study, through an *in vitro* growth inhibition screening of our fraction library against the NCI-60 SKOV3 human tumor cell line, we identified an actinomycete isolated from sediment collected off the Cát Bà peninsula in the East Sea of Vietnam. From this strain we isolated and characterized the novel diterpene isopimara-2-one-3-ol-8,15-diene (**1**) and lagumycin B (**2**), an angucycline that has yet to receive full structural characterization in the peer-reviewed literature (Figure 1) [7]. In addition, we identified the previously reported angucyclines dehydrorabelomycin (**3**) [8,9], phenanthroviridone (**4**) [10,11], and WS-5995 A (**5**) [12,13]. Herein we present the structure elucidation and biological activity of these compounds.

2. Results and Discussion

2.1. Structure Elucidation of Isopimara-2-one-3-ol-8,15-diene (1) and Lagumycin B (2)

Following a series of chromatographic experiments, **1** was obtained as a colorless solid. Combined HRMS and NMR experiments allowed for the assignment of the molecular formula as $C_{20}H_{30}O_2$, indicative of six degrees of unsaturation. ^1H and ^{13}C NMR data are shown in Table 1. In the ^1H NMR spectrum, we observed evidence for four sp^3 quaternary carbon-bound methyl groups, one vinyl group, an oxymethine geminal to a hydroxy group, a pair of geminal hydrogens adjacent to a carbonyl, and

additional methylene and methine groups on **1** that constituted the remainder of a pimarane diterpene core skeleton.

Table 1. ^{1}H and ^{13}C NMR data ($CDCl_3$) of **1**.

Position	^{13}C, Type [a]	^{1}H, Mult. (*J*, Hz) [b,c]
1_{ax}	49.8, CH_2	2.25, d (12.3)
1_{eq}		2.58, d (12.3)
2	211.8,C	
3	83.0, CH	3.91, d (4.0)
3-OH		3.44, d (4.0)
4	45.3, C	
5	50.3, CH	1.78, m
6	18.8, CH_2	1.58, m
		1.80, m
7	32.3, CH_2	2.03, m
8	126.4, C	
9	134.3, C	
10	43.8, C	
11_{ax}	21.4, CH_2	1.76, m
11_{eq}		1.88, m
12_{eq}	34.8, CH_2	1.33, m
12_{ax}		1.53, m
13	35.3, C	
14	41.6, CH_2	1.76, m
		1.88, m
15	145.9, CH	5.72, dd (17.5, 10.7)
16	111.2, CH_2	4.85, dd (17.5, 1.4)
		4.92, dd (10.7, 1.4)
17	28.3, CH_3	0.98, s
18	20.6, CH_3	0.93, s
19	29.3, CH_3	1.21, s
20	16.5, CH_3	0.72, s

[a] 226.2 MHz; [b] 600 MHz; [c] s = singlet; d = doublet; dd = doublet of doublets; m = multiplet.

Analysis of ^{13}C- DEPTQ and HSQC NMR data for **1** indicated the presence of one carbonyl carbon (δ_C 211.8, C-2), two fully-substituted endocyclic alkene carbons (δ_C 126.4, C-8; 134.3, C-9), one vinyl methylene carbon (δ_C 111.2, C-16), one vinyl methine carbon (δ_C 145.9, C-15), one oxymethine carbon (δ_C 83.0, C-3), and fourteen additional sp^3 carbons. Given that the molecular formula of **1** afforded six degrees of unsaturation and the molecule contained one carbonyl, one vinyl, and one endocyclic alkene group, the remaining three degrees were satisfied by the tricyclic pimarane ring system. Key HMBC, COSY, and 1D-TOCSY correlations are given in Figure 2.

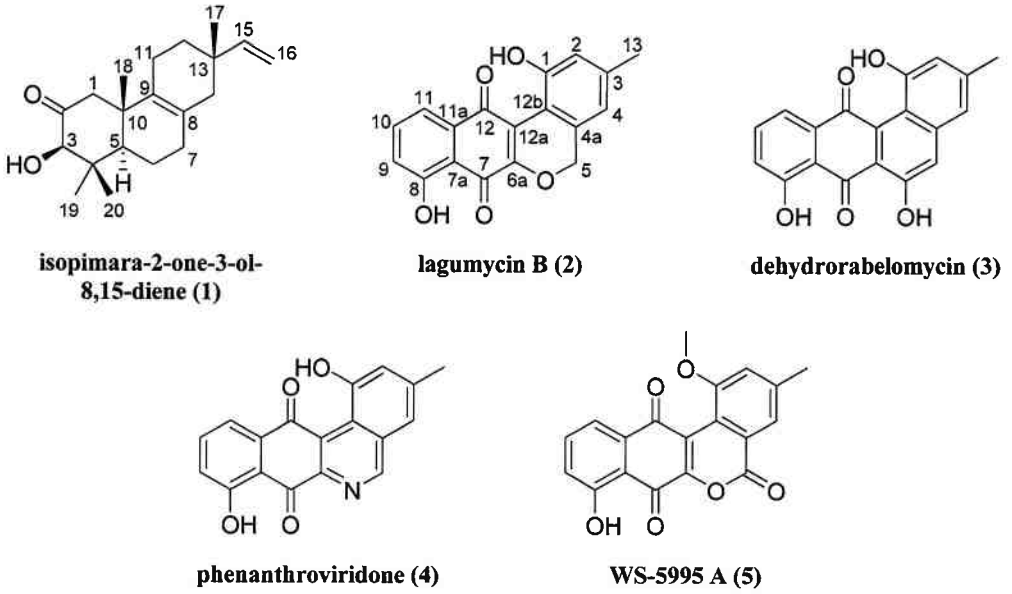

Figure 1. Structures of compounds **1**–**5**.

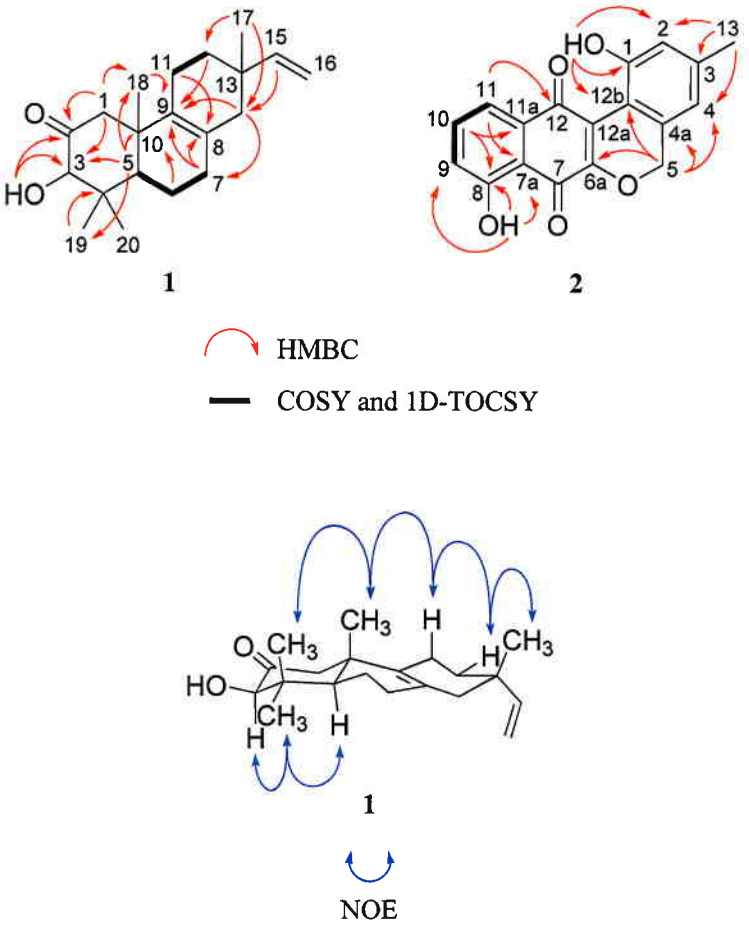

Figure 2. Key 2D NMR correlations of **1** and **2**.

The connectivity of the two distinct spin systems of C-11–C-12 and C-5–C-6–C-7 was determined by interpretation of the COSY NMR spectrum. Confirmation of these assignments was supported by a series of 1D-TOCSY experiments that exploited the solvent effect of C_6D_6 on lower frequency chemical shifts, which served to deconvolute the signal overlap observed when ^{1}H NMR experiments were run in $CDCl_3$ (Table S2 and Figures S5–S8) [14]. At this point in the elucidation process, we used HMBC correlations of methyl groups in **1** to piece together the tricyclic diterpene core. Geminal methyl groups were confirmed at C-4 based on HMBC correlations from H_3-19 and H_3-20 to C-3, C-4, and C-5. Signal H_3-18 exhibited correlations to C-1, C-9, and C-10, suggesting a bond to the quaternary C-10. The connectivity of ring A was further established by observation of HMBC correlations from H_2-1 to C-3, C-5, C-9, C-10, and C-18, suggesting that this methylene was between the C-2 carbonyl and C-10. Additionally, the oxymethine signal (H-3) showed HMBC couplings to C-2, C-4, C-19, and C-20, while the hydroxy signal (3-OH) displayed correlations to C-2 and C-3. This supported that H-3 and 3-OH were connected to the same carbon, which was positioned between the carbonyl at C-2 and the quaternary C-4. Couplings were also observed from H-5 to C-4 and C-10, solidifying the fusion of rings A and B. The connectivity of the C-5–C-6–C-7 spin system from ring A to the remainder of the core was established by observation of HMBC correlations from H_2-7 to C-8 and C-9. Correlations from H_2-14 to C-7, C-8, C-9, C-12, C-15, and C-17 placed it between the alkene C-8 and quaternary C-13. Resonance H_3-17 showed HMBC correlations to C-12, C-13, C-14, and C-15, placing it at position 13. HMBC correlations between the vinyl methine hydrogen (H-15) and C-13, C-14, and C-17 supported this, while correlations from H_2-16 to C-15 and C-13 provided further evidence for connectivity of the vinyl group to C-13. The remaining connectivity of ring C was satisfied by HMBC correlations from H_2-11 to C-8, C-9, and C-13.

A 2D-NOESY NMR experiment was employed in order to determine the relative stereochemistry of **1**, revealing correlations between H_3-20 and H_3-18, H_3-18 and H-11$_{ax}$, H-11$_{ax}$ and H-12$_{eq}$, and H-12$_{eq}$ and H_3-17; this suggested that these hydrogens projected out from the same face of the molecule. This orientation was supported by the observation of NOESY correlations between hydrogens H-3 and H_3-19, and H_3-19 and H-5, projecting from the opposite face of the molecule (Figure 2).

To identify the absolute configuration of centers in **1**, a CD spectrum was acquired and analyzed (Figure S11). Compound **1** exhibited a positive Cotton effect at the $n \rightarrow \pi^*$ carbonyl transition of 290 nm, indicating that the β-axial methyl group (C-18) was in the rear upper left octant when the octant rule was applied [15]. Thus, the absolute configuration of stereocenters in **1** was elucidated as 3*R*, 5*R*, 10*S*, and 13*S*, establishing the structure of **1** as shown.

Following a series of chromatographic steps, **2** was obtained as a pale orange solid. Combined HRMS and NMR experiments allowed for the assignment of the molecular formula as $C_{18}H_{12}O_5$, indicative of thirteen degrees of unsaturation. The UV absorption profile (maxima of 204, 280, 310, and 410 nm) of **2** displayed characteristics of an extended aromatic ring system similar to the previously reported angucycline isolates **3**, **4**, and **5**. ^{1}H and ^{13}C NMR data are shown in Table 2. A singlet resonance at δ_H 5.19 (2H, H-5) observed in the ^{1}H NMR spectrum indicated the presence of oxygenated methylene protons. Two highly deshielded resonances at δ_H 10.45 (1H, 1-OH) and δ_H 11.70 (1H, 8-OH) gave evidence of two hydroxy peri-protons. The observation of three aromatic signals at δ_H 7.30 (1H, H-9), δ_H 7.81 (1H, H-11), and δ_H 7.66 (1H, H-10) indicated the presence of a tri-substituted aromatic ring. Additionally, two singlet resonances were observed in the aromatic region at δ_H 6.54 (1H, H-4) and

δ_H 6.85 (1H, H-2), indicating the presence of isolated hydrogens on a separate, tetrasubstituted aromatic system. Finally, a singlet resonance at δ_H 2.33 (3H, H_3-13) evidenced one aromate-bound methyl group.

Analysis of ^{13}C-DEPTQ NMR data suggested the presence of two quinone carbonyls (δ_C 186.6, C-12; 183.4, C-7), two hydroxy-substituted aromatic carbons (161.7, C-8; 154.5, C-1), one oxygenated methylene carbon (δ_C 70.7, C-5), one methyl carbon (δ_C 21.3, H_3-13), and an additional twelve aromatic carbons. Given that the molecular formula afforded thirteen degrees of unsaturation and the molecule contained two carbonyls and seven double bonds, the remaining degrees were satisfied by the fused angucycline ring system.

Interpretation of COSY NMR data defined one distinct aromatic spin system that connected C-9–C-10–C-11, supporting the aforementioned evidence for a 1,2,3-trisubstitued benzene moiety. A phenolic hydroxy peri-proton at δ_H 11.70 showed HMBC correlations to C-7a, C-8, and C-9, establishing hydroxy connectivity to C-8. An aromatic hydrogen at H-10 exhibited an HMBC correlation to C-11a, completing assignments for the 1,2,3-trisubstitued benzene. An HMBC correlation observed between aromatic hydrogen H-11 and the carbonyl C-12 was critical to establishment of the phenol position relative to the central quinone ring. The positions of the C-7 and C-12 relative to the oxygenated carbon at C-6a were based on comparison to previously reported ^{13}C chemical shift values of similarly substituted paraquinones [16,17]. The 1-OH peri-proton showed HMBC correlations to C-1, C-12b, and C-2, providing evidence for connectivity of the hydroxy group to C-1. The singlet aromatic methyl signal at H_3-13 exhibited correlations to C-3, C-2, and C-4 in the HMBC spectrum, placing it *meta* to the hydroxy group at C-1. HMBC correlations from the oxygenated methylene at H_2-5 to C-4a, C-4, C-12b, and C-6a established connectivity of the naphthoquinone fragment to the phenol moiety. Key COSY and HMBC correlations are given in Figure 2. Thus, the structure of **2** is as shown with the name lagumycin B, following the structure and nomenclature established in the 1995 dissertation by Balk-Bindseil and Laatsch [7].

The characterization of known compounds **3–5** was based on comparison of ^{1}H NMR and HRMS data with those appearing in literature (Figures S18–S23) [8–13].

Table 2. ^{1}H and ^{13}C NMR data ($CDCl_3$) of **2**.

Position	^{13}C, Type [a]	^{1}H, Mult. (*J*, Hz) [b,c]
1	154.5, C	
1-OH		10.45, s
2	121.1, CH	6.85, s
3	143.7, C	
4	118.2, CH	6.54, s
4a	130.3, C	
5	70.7, CH_2	5.19, s
6a	157.0, C	
7	183.4, C	
7a	113.5, C	
8	161.7, C	
8-OH		11.70, s
9	125.2, CH	7.30, d (8.1)

Table 2. *Cont.*

10	137.2, CH	7.66, t (8.1)
11	121.3, CH	7.81, d (8.1)
11a	132.2, C	
12	186.6, C	
12a	124.4, C	
12b	109.9, C	
13	21.3, CH_3	2.33, s

[a] 226.2 MHz; [b] 600 MHz; [c] s = singlet; d = doublet; t = triplet.

*2.2. Cytotoxicity Evaluation of **1–5***

Following their identification, compounds **1–5** were assessed for cytotoxicity in two high-grade ovarian cancer cell lines, OVCAR4 and Kuramochi [18]. Potential for selective cytotoxicity was evaluated using two non-cancerous mouse cell lines representing the putative progenitor cells of ovarian cancer, murine ovarian surface epithelial (MOSE) and murine oviductal epithelial (MOE). Screening of **1–5** against this panel revealed **3** and **4** to be non-specifically cytotoxic, which was in accord with their previously reported bioactivities [8,10,11,19–21]. Compound **2** exhibited up to 14-fold enhanced cytotoxicity against non-cancerous murine cell lines MOSE and MOE, with LC_{50} values of 9.80 μM and 10.8 μM, respectively. Generally speaking, this para-quinone scaffold is not an attractive lead, as higher toxicity in non-tumorigenic cell lines confers serious overall toxicity. In contrast, compound **5** showed approximately seven-fold greater activity toward Kuramochi ovarian cancer cells with an LC_{50} of 18.6 μM (Table 3). Previous studies reported that **5** inhibits tumor cell proliferation and viability in L1210 lymphocytic leukemia cells *in vitro* with an IC_{50} range of 0.24–0.65 μM [22]. Compound **1** was not significantly active in all bioassays in the current study.

Table 3. *In vitro* cytotoxicity of **1–5**.

Compound	Cytotoxicity LC_{50} (μM) [a]			
	Kuramochi	OVCAR4	MOSE	MOE
1	>33.1	>33.1	>33.1	>33.1
2	>32.5	>32.5	9.80	10.8
3	6.72	11.0	3.50	28.5
4	1.11	4.82	2.85	6.20
5	18.6	127	>149	>149

[a] Doxorubicin was used as the positive control and was lethal at the lowest concentration tested (0.078 μM).

Compounds **2–5** are classified as angucyclines, which are among the largest class of type II PKS natural products and are known to exhibit a wide variety of biological activities [23]. Compound **2** was initially isolated from marine *Streptomyces* sp. B8245 and reported in a dissertation, but it has yet to receive formal characterization [7]. Both **3** and **4** have previously been identified as intermediates in kinamycin biosynthesis [24,25]; this product was not detected in our fermentation extracts. Similarly, compound **3** was proven to be a biosynthetic intermediate of jadomycin and gilvocarcin in a *Streptomyces lividans* strain [26], though these were also not observed in secondary metabolite fractions produced by our *Micromonospora* strain. In previous reports, **3** exhibited no detectable activity when

screened against a panel of Gram-negative and Gram-positive bacteria [27], but inhibited a wide range of cancer cell lines at micromolar potency. Compound **4** was reported to have a variety of antibiotic and cytotoxic properties and our data support these non-specific biological activities [10,11,21]. Finally, compound **5** was first isolated from a *Streptomyces auranticolor* strain and was reported to exhibit anticoccidial activity against the apicomplexan poultry parasite *Eimeria tenella*, while exhibiting no significant biological activity when screened against a panel that included two fungal species, a human parasite, and several Gram-negative and Gram-positive bacteria [12,13]. This compound was also studied more recently for its aforementioned antileukemic activity, where it inhibited proliferation leading to apoptosis through DNA cleavage, blockage of nucleoside transport and inhibition of DNA, RNA, and protein synthesis [22]. To our knowledge, this study is the first to report cytotoxicity of compound **5** in carcinomas. In most cases, **4** is significantly more cytotoxic than **3** and **5**. Presumably, this is due to the pyridine function in **4**. Additionally, a contributing factor to reduced cytotoxicity may be the loss of aromaticity in the adjacent anthraquinone ring (**5**), though further biological testing and structure activity analyses are required to support this.

3. Experimental Section

3.1. General Experimental Procedures

Optical rotation measurement was performed in MeOH using a 10.0 cm cell on a PerkinElmer 241 polarimeter at 25 °C. The UV spectra were measured on a Shimadzu Pharma Spec UV-1700 spectrophotometer. NMR spectra were obtained on a Bruker 600 MHz DRX NMR spectrometer equipped with an inverse 5 mm TXI cryogenic probe with z-axis pfg and XWINNMR version 3.5 operating software, and a 900 (226.2) MHz Bruker AVANCE NMR spectrometer equipped with an inverse 5 mm TCI cryogenic probe with z-axis pfg and TopSpin version 1.3 operating software at the University of Illinois at Chicago Center for Structural Biology. Chemical shifts (δ) are given in ppm and coupling constants (*J*) are reported in Hz. ^{1}H and ^{13}C NMR resonances of **1** and **2** are reported in Tables 1 and 2, respectively. ^{1}H and ^{13}C NMR chemical shifts were referenced to the $CDCl_3$ (δ_H 7.26 ppm and δ_C 77.0 ppm, respectively) and C_6D_6 solvent signals (δ_H 7.16 ppm and δ_C 128.1 ppm, respectively). High resolution mass spectra were obtained on a Waters Synapt QToF mass spectrometer at the University of Illinois at Chicago Research Resources Center (UIC RRC). High-performance liquid chromatography (HPLC-UV) data were obtained using a Hewlett-Packard series 1100 system controller and pumps with a Model G1315A diode array detector (DAD) equipped with a reversed-phase C_{18} column (Phenomenex Luna, 100 mm × 4.6 mm, 5 μm; Torrance, CA, USA) at a flow rate of 0.5 $mL \cdot min^{-1}$. Semi-preparative HPLC scale separations were performed using a Hewlett Packard Series 1050 system with a Phenomenex Luna semi-preparative C_{18} column (250 mm × 10 mm, 5 μm) at a flow rate of 2.4 $mL \cdot min^{-1}$. Preparative HPLC scale separations were performed using a Waters LC4000 System equipped with a Phenomenex Luna preparative C_{18} column (250 mm × 21.2 mm, 5 μm) at a flow rate of 16 $mL \cdot min^{-1}$. Silica gel column chromatography was conducted using Bonna-Angela Technologies Cleanert® silica gel (Wilmington, DE, USA) with an average particle size of 40–60 μm and an average pore size of 60 Å.

3.2. Collection and Identification of Actinomycete Strain G039

Strain G039 was isolated from a sediment sample collected by PONAR at a depth of 22 m, from *ca.* 3.3 miles off the coast southeast of Cát Bà Peninsula in Vietnam (20°41′30″ N, 107°05′58″ E) in July of 2011. Strain G039 (GenBank accession number KR703606) shared 99% 16S rRNA gene sequence identity with the type strain *Micromonospora haikouensis* (GenBank accession number NR117442) [28].

3.3. Fermentation and Extraction

Strain G039 was grown in 38 × 1 L portions in Fernbach flasks containing high nutrient media components in artificial seawater (10 g starch, 4 g yeast extract, 2 g peptone, 1 g calcium carbonate, 100 mg potassium bromide, 40 mg iron sulfate, and 33.3 g Instant Ocean® (Blacksburg, VA, USA) per liter of dH_2O) for 7 days at 21 °C while shaking at 220 rpm. Sterilized Amberlite XAD-16 resin (15 $g \cdot L^{-1}$) was added to each flask to absorb the extracellular secondary metabolites. The culture medium and resin were shaken for 10 h and filtered using cheesecloth to remove the resin. The resin, cell mass, and cheesecloth were extracted with acetone overnight, concentrated under vacuum, and partitioned between water and ethyl acetate. The organic layer was dried under vacuum to afford 3.52 g of extract.

*3.4. Isolation and Characterization of Isopimara-2-one-3-ol-8,15-diene (**1**) and Lagumycin B (**2**)*

The organic layer from the liquid-liquid partition was fractionated using silica gel flash column chromatography (23 cm × 3.5 cm, 85 g silica) eluting with a step gradient solvent system of 200 mL 100% hexanes (HEX), 200 mL 90% HEX:10% dichloromethane (DCM), 200 mL 70% HEX:30% DCM, 200 mL 100% DCM, 200 mL 70% DCM:30% ethyl acetate (EtOAc), 200 mL 70% EtOAc:30% DCM, 200 mL 100% ethyl acetate, 200 mL 95% EtOAc:5% 2-propanol, 200 mL 90% EtOAc:10% methanol (MeOH), 200 mL 50% EtOAc:50% MeOH, 400 mL 95% MeOH:5% ammonium hydroxide (NH_4OH) to afford eleven fractions. Upon re-screening, it was determined that fraction 3 contained the bioactive constituents, thus, it was further separated using RP-C_{18} preparative HPLC (16 $mL \cdot min^{-1}$, gradient of 50% aqueous MeOH to 100% MeOH over 25 min, followed by an isocratic flow of 100% MeOH for 15 min), to afford 13 fractions. Fractions 6 and 11 exhibited biological activity so they were further separated.

Fraction 6 was further purified using RP-C_{18} semi-preparative HPLC (2.4 $mL \cdot min^{-1}$, gradient of 70% aqueous MeOH to 80% MeOH for 37.5 min, followed by an isocratic flow of 100% ACN for 10 min) to afford phenanthroviridone (**4**, t_R 37.5 min, 0.66 mg, 0.019% yield), lagumycin B (**2**, t_R 40.2 min, 0.9 mg, 0.026% yield) and WS-5995 A (**5**, t_R 42.0 min, 1.2 mg, 0.034% yield).

Fraction 11 was further separated using RP-C_{18} semi-preparative HPLC (2.4 $mL \cdot min^{-1}$, gradient of 80% aqueous MeOH to 90% MeOH for 37.5 min, followed by an isocratic flow of 100% ACN for 10 min) to afford 8 fractions. Fraction 2 was further purified using two iterations of RP-C_{18} semi-preparative HPLC (2.4 $mL \cdot min^{-1}$, gradient of 80% aqueous MeOH to 90% MeOH for 37.5 min, followed by an isocratic flow of 100% ACN for 10 min) to afford dehydrorabelomycin (**3**, t_R 26.7 min, 0.4 mg, 0.011% yield). Purification of compound **3** also afforded isopimara-2-one-3-ol-8,15-diene (**1**, t_R 27.5 min, 0.9 mg, 0.026% yield), eluting as a neighboring peak observable at 220 nm.

Isopimara-2-one-3-ol-8,15-diene (**1**): Colorless solid (0.9 mg). $[\alpha]_D^{25} = +20.7$ (c = 0.00053, MeOH). UV (MeOH) λ_{max} (log ε) = 204 (3.67) and shoulders at 228 (3.39) and 242 (3.30) nm. CD (c = 0.0031,

MeOH): λ_{max} ($\Delta\varepsilon$) = 225 (+65.2), 250 (−4.4), 290 (+54.4) nm (Figure S11). ^{1}H NMR (900 MHz, $CDCl_3$) and ^{13}C NMR (226.2 MHz, $CDCl_3$), see Table 1. HRESI-QToF MS *m/z* 303.2338 $[M + H]^+$ (calcd. for $C_{20}H_{31}O_2$: 303.2319), and *m/z* 325.2141 $[M + Na]^+$ (calcd. for $C_{20}H_{30}O_2Na$: 325.2138).

Lagumycin B (**2**): Pale orange solid (0.9 mg). UV (MeOH) λ_{max} (log ε) = broad absorptions with maxima at 204 (3.57), 280 (2.86), 310 (2.73) and 410 (2.27) nm. ^{1}H NMR (600 MHz, CDCl3) and ^{13}C NMR (226.2 MHz, $CDCl_3$), see Table 2. HRESI-QToF MS *m/z* 309.0773 $[M + H]^+$ (calcd. for $C_{18}H_{13}O_5$: 309.0757).

3.5. OVCAR4, Kuramochi, MOSE, MOE, and Vero Cytotoxicity Assays

Human ovarian OVCAR4 and Kuramochi cancer cells were maintained in RPMI 1640 (11875-093, Life-technologies; Carlsbad, CA, USA) supplemented with 10% FBS (16000-044, Life-technologies; Carlsbad, CA, USA) and 1% penicillin/streptomycin. Non-cancerous murine ovarian surface epithelium (MOSE) and murine oviductal epithelium (MOE) cells were maintained as previously reported [29]. Concentration-response experiments were performed as previously described for 72 h [6].

4. Conclusions

Of the five compounds isolated in this study, two were previously unreported. Compound **1** represents a relatively rare example of the isolation of a diterpene from an actinomycete strain. Since a previous report that mined the genomes of a small population of actinomycete strains suggested that this phylum has a far greater capacity to produce diterpenes (25 of 100 strains) than is represented in the peer reviewed literature, it is possible that this discrepancy is a product of these pathways remaining silent under laboratory growth conditions, or of the methods used to isolate natural products from bacteria, namely bioassay-guided fractionation [3]. One possible explanation of the latter phenomenon is that specific classes of diterpenes are conserved within Actinobacteria, and that these classes are not biologically active in the typical barrage of assays used to discover small molecule leads, though in the absence of extensive genome mining and subsequent structure identification-bioactivity experiments, this will remain speculation.

The novel diterpene isopimara-2-one-3-ol-8,15-diene (**1**) was isolated along with the angucycline lagumycin B (**2**), and three other angucyclines from a *Micromonospora* sp. collected in the East Sea of Vietnam. The angucyclines exhibited varying degrees of cytotoxicity against a panel of cancerous and non-cancerous cell lines, with the notable exception of WS-5995 A (**5**), which showed enhanced cytotoxicity against the Kuramochi cell line when compared to non-tumorigenic cell lines. Though not significantly active in our bioassays, the discovery of isopimara-2-one-3-ol-8,15-diene contributes to the growing but still relatively small number of diterpenes identified from actinomycetes. This study highlights our collaborative efforts to discover novel biologically active molecules from the large, underexplored, and biodiversity-rich waters of Vietnam's East Sea.

Acknowledgments

The authors would like to acknowledge the Institute of Marine Environment and Resources at VAST for assistance in sample collection; Ying Gao, Mark Sadek, Skylar Carlson, and Maryam Elfeki for fraction library development and preliminary bioactivity screening of strain G039; Baojie Wan, Sanghyun Cho, and Scott G. Franzblau of the Institute for Tuberculosis Research (ITR) at the University of Illinois at Chicago for initial screening of strain G039 against Mycobacterium tuberculosis; Dejan Nikolic of the University of Illinois at Chicago Research Resources Center (UIC RRC) for assistance in acquisition of mass spectra; David Lankin for assistance in acquiring ^{13}C-DEPTQ NMR and 1D-TOCSY NMR data, and Benjamin E. Ramirez and Gerd Prena of the University of Illinois at Chicago Center for Structural Biology (UIC CSB) for assistance in acquiring remaining NMR data and CD spectroscopic data, respectively. This project was funded under Department of Defense grant #W81XWH-13-1-0171, UIC Campus Research Board grant, and American Cancer Society (Illinois Division) grant #254871. MWM is supported by the Office of the Director, National Institutes of Health (OD) and National Center for Complementary and Integrative Health (NCCIH) (5T32AT007533). The authors also acknowledge the Ministry of Science and Technology of Vietnam (MOST) and the Vietnam Academy of Science and Technology (VAST) for financial support (Grant No.: VAST.TĐ.ĐAB.04/13-15).

Author Contributions

Conceived and designed the experiments: MWM, EÓ, JB, VCP, BTM. Performed the experiments: MWM, EÓ, UT, VCP, BTM. Analyzed the data: MWM, EÓ, JB, BTM. Wrote the paper: MWM, EÓ, JB, BTM.

Conflicts of Interest

The authors declare no conflict of interest.

References

1. Fenical, W.; Jensen, P.R. Developing a new resource for drug discovery: Marine actinomycete bacteria. *Nat. Chem. Biol.* **2006**, *2*, 666–673.
2. Newman, D.J.; Cragg, G.M. Natural products as sources of new drugs over the 30 years from 1981 to 2010. *J. Nat. Prod.* **2012**, *75*, 311–335.
3. Xie, P.; Ma, M.; Rateb, M.E.; Shaaban, K.A.; Yu, Z.; Huang, S.-X.; Zhao, L.-X.; Zhu, X.; Yan, Y.; Peterson, R.M.; *et al.* Biosynthetic potential-based strain prioritization for natural product discovery: A showcase for diterpenoid-producing actinomycetes. *J. Nat. Prod.* **2014**, *77*, 377–387.
4. Smanski, M.J.; Peterson, R.M.; Huang, S.-X.; Shen, B. Bacterial diterpene synthases: New opportunities for mechanistic enzymology and engineered biosynthesis. *Curr. Opin. Chem. Biol.* **2012**, *16*, 132–141.
5. Mullowney, M.W.; Hwang, C.H.; Newsome, A.G.; Wei, X.; Tanouye, U.; Wan, B.; Carlson, S.; Barranis, N.J.; Ó hAinmhire, E.; Chen, W.-L.; *et al.* Diaza-anthracene antibiotics from a freshwater-derived actinomycete with selective antibacterial activity toward *Mycobacterium tuberculosis*. *ACS Infect. Dis.* **2015**, *1*, 168–174.

6. Mullowney, M.W.; Ó hAinmhire, E.; Shaikh, A.; Wei, X.; Tanouye, U.; Santarsiero, B.D.; Burdette, J.E.; Murphy, B.T. Diazaquinomycins E–G, novel diaza-anthracene analogs from a marine-derived *Streptomyces* sp. *Mar. Drugs* **2014**, *12*, 3574–3586.
7. Balk-Bindseil, W.; Laatsch, H. Neue Naturstoffe aus dem Screening Mariner Actinomyceten: Isolierung und Strukturaufklärung der Lagumycine und des Oceamycins. Ph.D. Thesis, University of Göttingen, Göttingen, Germany, 1995.
8. Yamashita, N.; Takashi, H.; Kazuo, S.; Haruo, S. 6-Hydroxytetrangulol, a new CPP32 protease inducer produced by *Streptomyces* sp. *J. Antibiot.* **1998**, *1*, 79–81.
9. Liu, W.C.; Parker, L.; Slusarchyk, S.; Greenwood, G.L.; Grahm, S.F.; Meyers, E. Isolation, characterization, and structure of rabelomycin, a new antibiotic. *J. Antibiot.* **1970**, *23*, 437–441.
10. Fendrich, G.; Zimmermann, W.; Gruner, J.; Auden, J.A.L. Phenanthridine Derivatives, Process for the Preparation Thereof, and Compositions Containing Them. U.S. Patent 5,093, 3 March 1990.
11. Gore, M.P.; Gould, S.J.; Weller, D.D. Synthesis of putative intermediates in the biosynthesis of the kinamycin antibiotics: Total synthesis of phenanthroviridin aglycon and related compounds. *J. Org. Chem.* **1992**, *57*, 2774–2783.
12. Ikushima, H.; Iguchi, E.; Kohsaka, M.; Aoki, H.; Imanaka, H. *Streptomyces auranticolor* sp. nov., a new anticoccidial antibiotics producer. *J. Antibiot.* **1980**, *33*, 1103–1106.
13. Ikushima, H.; Okamoto, M.; Tanaka, H.; Ohe, O.; Kohsaka, M.; Aoki, H.; Imanaka, H. New anticoccidial antibiotics, WS-5995 A and B: I. Isolation and characterization. *J. Antibiot.* **1980**, *33*, 1107–1113.
14. Crews, P.; Rodríguez, J.; Jaspars, M. *Organic structure Analysis*, 2nd ed.; Oxford University Press: New York, NJ, USA, 2010; p. 48.
15. Moffitt, W.; Woodward, R.B.; Moscowitz, A.; Klyne, W.; Djerassi, C. Structure and the optical rotatory dispersion of saturated ketones. *J. Am. Chem. Soc.* **1961**, *83*, 4013–4018.
16. Dawson, B.A.; Girard, M.; Kindack, D.; Fillion, J.; Awang, D.V.C. ^{13}C NMR of lapachol and some related naphthoquinones. *Magn. Reson. Chem.* **1989**, *27*, 1176–1177.
17. Yamashita, M.; Kaneko, M.; Tokuda, H.; Nishimura, K.; Kumeda, Y.; Iida, A. Synthesis and evaluation of bioactive naphthoquinones from the Brazilian medicinal plant, *Tabebuia avellanedae*. *Bioorg. Med. Chem.* **2009**, *17*, 6286–6291.
18. Domcke, S.; Sinha, R.; Levine, D.A.; Sander, C.; Schultz, N. Evaluating cell lines as tumour models by comparison of genomic profiles. *Nat. Commun.* **2013**, *4*, 1–10.
19. Lombó, F.; Abdelfattah, M.S.; Braña, A.F.; Salas, J.A.; Rohr, J.; Méndez, C. Elucidation of oxygenation steps during oviedomycin biosynthesis and generation of derivatives with increased antitumor activity. *ChemBioChem* **2009**, *10*, 296–303.
20. Yamashita, N. Manufacture of Dehydrorabelomycin with *Streptomyces* Species and Use of the Antibiotic Agent as Antitumor Agent. JP 10201494 A, 4 August 1998.
21. Zhang, W.; Liu, Z.; Li, S.; Lu, Y.; Chen, Y.; Zhang, H.; Zhang, G.; Zhu, Y.; Zhang, G.; Zhang, W.; *et al.* Fluostatins I–K from the South China Sea-derived *Micromonospora rosaria* SCSIO N160. *J. Nat. Prod.* **2012**, *75*, 1937–1943.

22. Perchellet, E.M.; Sperfslage, B.J.; Qabaja, G.; Jones, G.B.; Perchellet, J.P. Quinone isomers of the WS-5995 antibiotics: Synthetic antitumor agents that inhibit macromolecule synthesis, block nucleoside transport, induce DNA fragmentation, and decrease the growth and viability of L1210 leukemic cells more effectively than ellagic acid and genistein *in vitro*. *Anticancer Drugs* **2001**, *12*, 401–417.
23. Kharel, M.K.; Pahari, P.; Shepherd, M.D.; Tibrewal, N.; Nybo, S.E.; Shaaban, K.A.; Rohr, J. Angucyclines: Biosynthesis, mode-of-action, new natural products, and synthesis. *Nat. Prod. Rep.* **2012**, *29*, 264–325.
24. Seaton, P.J.; Gould, S.J. Kinamycin biosynthesis. Derivation by excision of an acetate unit from a single-chain decaketide intermediate. *J. Am. Chem. Soc.* **1987**, *109*, 5282–5284.
25. Cone, M.C.; Hassan, A.M.; Gore, M.P.; Gould, S.J.; Borders, D.B.; Alluri, M.R. Detection of phenanthroviridin aglycon in a UV mutant of *Streptomyces murayamaensis*. *J. Org. Chem.* **1994**, *59*, 1923–1924.
26. Tibrewal, N.; Pahari, P.; Wang, G.; Kharel, M.K.; Morris, C.; Downey, T.; Hou, Y.; Bugni, T.S.; Rohr, J. Baeyer–Villiger C–C bond cleavage reaction in gilvocarcin and jadomycin biosynthesis. *J. Am. Chem. Soc.* **2012**, *134*, 18181–18184.
27. Cone, M.C.; Seaton, P.J.; Halley, K.A.; Gould, S.J. New products related to kinamycin from *Streptomyces murayamaensis*. I. Taxonomy, production, isolation, and biological properties. *J. Antibiot.* **1989**, *42*, 179–188.
28. Xie, Q.Y.; Qu, Z.; Lin, H.P.; Li, L.; Hong, K. *Micromonospora haikouensis* sp. nov., isolated from mangrove soil. *Antonie Leeuwenhoek* **2012**, *101*, 649–655.
29. Ó hAinmhire, E.; Quartuccio, S.M.; Cheng, W.; Ahmed, R.A.; King, S.M.; Burdette, J.E. Mutation or loss of p53 differentially modifies TGFβ action in ovarian cancer. *PLoS ONE* **2014**, *9*, doi:10.1371/journal.pone.0089553.